# Assessing the impact of a large multi-purpose reservoir on flood control under moderate and extreme flood conditions

Pratik Chakraborty[a]*, Sophie De Kock[b], Pierre Archambeau[a], Michel Pirotton[a], Sébastien Erpicum[a] and Benjamin Dewals

*[a]Hydraulics in Environmental and Civil Engineering (HECE), University of Liège (ULiège), Liège, Belgium; [b]Geotechnical Engineering, University of Liège (ULiège), Liège, Belgium*

*Corresponding author:
Pratik Chakraborty
p.chakraborty@uliege.be
Bat. B52/3 Hydraulics in Environmental and Civil Engineering
Quartier Polytech 1
Allée de la Découverte 9
4000 Liège 1
Belgique

# Assessing the impact of a large multi-purpose reservoir on flood control under moderate and extreme flood conditions

This study offers a detailed examination of the Eupen dam's role in flood mitigation in Belgium's Vesdre valley, analysing 18 moderate and extreme flood events from 1995-2022. Notable aspects of the methodology include adjustments for an ungauged sub-basin and a mass-balance approach to compute the unknown outflow data from the inflow time-series and reservoir level data. These 18 events evidence the dam's performance hitherto, with respect to peak discharge attenuation (9-91%), peak delay (0-68 hours), outflow volume reduction (2-94%), as well as discharge reductions associated with various return periods (38-51%), given its multipurpose objectives. The research details how the dam's effectiveness varies with operational decisions and antecedent reservoir conditions, marking a departure from conventional studies that tend to generalise data across multiple dams and events. By focusing on individual events, the study provides insights into the nuanced interplay between dam operations and flood management, demonstrating the benefits and limitations of multi-purpose reservoirs in flood control.

Keywords: flood risk; flood control; extreme events; large reservoir; dam operation

## 1. Introduction

### *1.1 Background*

Dams are one of the most emblematic hydraulic structures around the world. In providing critical functions such as water supply, hydroelectric power generation, and flood control, these structures fundamentally alter hydrological regimes. Key aspects of these changes include regulation of floods and base flows, and alteration in the seasonal and flood-related hydrograph characteristics (Batalla et al., 2004). Such changes are not only caused by the dynamic influence of the operating rules of the dam but may also be triggered by alterations in basin characteristics related to the dam installation, such as the construction of diversion channels to drain water from nearby catchments. The changes due to dam-operation, in turn, are dictated by the intended purpose of a dam (single-purpose dam) or the combination of purposes served by the dam (multi-purpose dams), such as flood control, drinking water supply, hydropower production etc. (Mailhot et al., 2018). For multi-purpose dams, the various services are ranked according to their levels of priority. This ranking plays a crucial role in dictating the dam's operational behaviour.

Dam reservoirs, whose purpose is to store water, in turn reduce annual peak discharge and the variability in mean daily discharge (Assani et al., 2006; Ely et al., 2020; Song et al., 2020). This reduction occurs due to decreased high flows and increased low flows, leading to flood wave modification. Additionally, dam operations can cause shifts in the timings of the flood peaks and corresponding lower flow rates. The scale of these shifts ranges typically from a couple of hours to a few days. However, these implications are not generic to all dams since each dam is uniquely designed, built, and operated for a purpose or a set of purposes (single- or multi-purpose dams) under unique conditions. Therefore, understanding the effects of a dam requires a holistic understanding of the context within which it is operated.

### *1.2 Literature review*

Table 1 reviews several studies in relation to the impacts of dams on streamflow characteristics. Against each study it is also indicated as to which aspects of the dam's effects were examined.

Most studies report quantitatively on peak reduction effects. Some studies majorly deal in annual statistics (Fantin-Cruz et al., 2015; Graf, 2006; Mei et al., 2017). For instance, Graf (2006) studied the hydrologic and geomorphic changes downstream of dams, analysing 36 large dams in the United States. Their findings included a significant reduction in average annual peak discharge (by 67%) and the ratio of annual max/mean flow (by 60%). Similarly, Mei et al. (2017) compared annual mean peak discharges across 38 U.S. rivers, observing a decrease ranging from 7 to 95%. Some other studies also discuss the effects of damming on flood events separately (Stecher & Herrnegger, 2022; Yun et al., 2020).

Strong focus has also been found to be on flood-frequency analysis and associated statistics. Mei et al. (2017) reported a significant reduction in flood discharges for various recurrence intervals - ranging from 41% to 47% for 2 to 50 years return period floods, while Stecher & Herrnegger (2022) found an average reduction of 23.5% for 10 to 30-year floods. Notably, they found that the flood peak reduction effect of the dams was more pronounced for return periods longer than 30 years (showing an average flood peak reduction of 33%). Another study by Yun et al. (2020) analysed such peak reduction in light of climate change effects. In parts of their study area, climate change was found to escalate flood magnitude by as much as 14% and frequency by approximately 45%. However, the operational management of reservoirs effectively mitigated these risks, diminishing flood magnitude and frequency by 16% and 36%, respectively.

A widely recognized set of metrics for assessing the impact of flow regulation is the Indicators of Hydrologic Alteration (IHA), introduced by Richter et al. (1996). Using various parameters, they describe the inter-annual as well as intra-annual variations in the flow regime due to regulation. Studies which utilized the IHA software programme, therefore, report on the alterations in the temporal characteristics of streamflow. This includes (among others) the timing of the annual extreme conditions and discharge gradients. For instance, Graf (2006) reported a delay (in the median date of annual maximum) of 0 days, while Fantin-Cruz et al. (2015) observed a 5-day delay.

Both studies also report a reduction in the rising rates of flood hydrographs. Apart from these studies, Rahman & Bowling (2019) also characterised such temporal tendency using the Richards-Baker Flashiness Index (Baker et al., 2004).

Batalla et al. (2004) added that the effect of a reservoir is a function of the operating rules of the dam. Complementing this, Mailhot et al. (2018) focused on identifying the role of dam operation in particular. They invoke the idea that multi-modal distributions in outflow time-series are indicative of regulation. This is plausible since natural flows are very likely to be unimodal or have low `non-unimodality'. Based on this, they proposed the use of the Degree of Regulation (DOR) metric (Lehner et al., 2011) and certain associated thresholds to evaluate regulation effects or its lack thereof. Given such influence of dam operation on the flow characteristics, studies have also focused on the development and application of different techniques to optimise the services derived from dams (Becker et al., 2023; Jordan et al., 2012).

From a methodological standpoint, it is often the case that in order to understand the impact of a dam, the natural flow regime of the river is compared to the altered one. This, however, may be conducted in different ways. Some studies compare flow time-series data from pre- and post-construction periods (Mei et al., 2017; Stecher & Herrnegger, 2022). However, it can be ambiguous as to how far the pre-construction hydrographs still hold true after the introduction of the dam. This ambiguity maybe linked with changes that are directly or indirectly associated with the construction of the dam. Direct changes include (and are not limited to) local topographical changes as well as long- and short-term geomorphological changes caused by the dam installation. On the other hand, indirect changes include developments that may follow the construction of a dam (socio-economic reorganisation and associated water utilisations).

A different approach could be based on the understanding that the `inflow discharge' to a dam also represents the ‘natural outflow rate’ i.e., flow-rate downstream if the dam did not exist. In that case, a comparison of the inflow and outflow time-series at the dam location could indicate its storage effects (Ayalew et al., 2013; Rahman & Bowling, 2019). Nonetheless, Terrier et al. (2021), in their review, state that there are broadly six different methods of naturalization, viz., (a) water balance, (b) reconstitution, (c) extension, (d) paired catchment, (e) regionalization, and (f) routing method. The adoption of a method depends strongly on the available data.

### *1.3 Objective*

This study embarks on a detailed, singular case analysis of the Eupen dam, located in the Vesdre valley (Belgium), which is distinct from the broader, often generalized approach seen in existing literature. Contrary to previous studies that predominantly focus on mean annual flow characteristics or aggregate data across numerous dams, the present investigation zeroes in on individual flood events associated with a single dam. This targeted approach allows for a more nuanced understanding of the dam's behaviour, offering a unique opportunity to closely examine the interplay of several aspects of the dam's storage effect on the streamflow characteristics.

## 2 Data and method

### *2.1 Case study*

The Eupen dam, positioned in Belgium's Walloon region at the Vesdre and Getzbach rivers' confluence, is the focal point of this study (Figure 1). Originating from the High Fens, the 70 km Vesdre river is a tributary of the Ourthe, which in turn feeds into the Meuse river.

### 2.1.1 Dam and catchment characteristics

Constructed in 1949, the concrete gravity dam of the reservoir serves multiple purposes. Its primary function is the provision of potable and industrial water. The reservoir, covering a 126-ha surface area, has a total storage capacity of 25 $Mm^3$ (Ministère des travaux publics, 1986) and has an impoundment index of 0.321 (Gutenson et al., 2020) i.e. about a third of the average annual inflow can be stored in the dam. It is also instrumental in managing flood risks and contributes modestly to hydroelectric power generation.

The dam's natural watershed spans an area of 65 $km^2$, which was further extended by 36.9 $km^2$ following the Helle river's diversion tunnel construction (Ministère des travaux publics, 1986). Typically, this tunnel remains open, maintaining a minimal environmental flow back to the Helle river although its discharge capacity is limited by construction to 10 $m^3/s$.

Another peculiarity of this basin is the diversion of the Vesdre river through a canal of the same name before it enters Germany. A part of the flow is diverted so that it remains on German territory. It is, therefore, important to discard the part of the flow (thereby, that catchment area) that is retained in the German territory anthropogenically. The 65 $km^2$ figure mentioned above is obtained after considering this subtraction.

### 2.1.2 Management of the dam

The operational strategy of the Eupen dam is closely linked to meteorological conditions, particularly past and anticipated rainfall. This is crucial for maintaining a balance between having ample water for community water supply and retaining sufficient reservoir capacity to manage sudden influxes of water.

The dam employs three primary mechanisms for water discharge (Ministère des travaux publics, 1986; Zeimetz et al., 2021):

(1) 4 turbines: One of the four turbines is used to transfer water to the drinking water treatment plant while the rest maybe used for electricity generation and water return to the river (maximum discharge: 4.5 $m^3/s$)
(2) 2 bottom outlet valves (each with a maximum discharge of 35 $m^3/s$)
(3) 1 surface spillway (2 gates), with the crest of the spillway at 358 m TAW (maximum discharge: 230 $m^3/s$).

As displayed in Figure 2, the reservoir operation is primarily governed by three key water levels:

- the 'target water level' (TWL, referred to as 'courbe de manutention' in French), which shows seasonal variations;
- the 'normal water level' (NWL), fixed at 358.5 m throughout the year, which designates the maximum level under normal operating conditions, exclusive of the provision for flood storage (ICOLD, 1994);
- and the 'maximum water level' (MWL), equal to 360.8 m, which refers to the maximum water level, including flood storage, which the dam has been designed to withstand (ICOLD, 1994). Should the reservoir water level exceed MWL, the operations change to a 'pass inflow' regime, i.e., all incoming water is released (Bruwier et al., 2015; Zeimetz et al., 2021).

The value of TWL varies within a year. During winter , the target water level is kept low to enable better accommodating incoming floods. On the other hand, the reservoir is to be filled in preparation for summer which is when low flow periods are more likely to occur. This filling season is clearly shorter (December 31st to January

31st) than the long and gradual drawdown from February 1st to December 31st (Figure 2).

The target water level depicted in Figure 2 is an operational approximation (with target levels for every 15 days or a month, within a year) with sharp jumps, especially in the filling season going from December to January. In reality, the transitions between different water levels follow more practicable gradients, as displayed in Figure A.1 in Appendix.

In normal operating conditions, the two spillway gates are maintained at NWL. The NWL was established to ensure that approximately 3 $Mm^3$ of free storage is available for flood storage. All 18 flood events considered in the present study bore inflow volumes greater (mean flood volume = 6.5 $Mm^3$) than this flood storage volume. More recently, the value of NWL has been reduced to ensure a higher free storage for flood mitigation; but this change has no influence on the analyses presented here since it is posterior to all the 18 considered flood events.

Depending on the relative value of the actual water level in the reservoir compared to TWL, NWL and MWL, different operation regimes may be distinguished. While the drinking water intake remains constant at 0.63 $m^3/s$ regardless of the operation regime, hydropower generation is varied as per the regime in place:

- When the actual water level in the reservoir falls beneath TWL (Regime A in Figure 2), only a minimum environmental flow (0.22 $m^3/s$) is released, and hydropower generation is interrupted.
- In Regime B, i.e., when the water level in the reservoir is in-between TWL and NWL, the operator is generally free to generate hydropower, up to the maximum capacity of the turbines (4.5 $m^3/s$, in Regime B2), except when the reservoir

level gets close to the TWL (Regime B1). In this case, hydropower generation is reduced.

- Under normal operating conditions, when the reservoir level exceeds NWL, the water level is brought back to the NWL by means of maximum hydropower production along with other releases, if necessary and permissible. In contrast, when an incoming flood moves into the rising limb of the hydrograph, spillway gates may be raised to achieve flood storage up to the MWL; but once the peak of the hydrograph is past, the reservoir level is to be brought back down to the NWL via gradual controlled releases.

## ***2.2 Data and processing***

### *2.2.1 Inflow discharge*

In calculating the total inflow into the Vesdre reservoir, it is essential to consider four primary sources: the Vesdre river, the Getzbach River, the diversion tunnel from the Helle River (Figure 3) and direct runoff from the surrounding catchment area.

Data for the Getzbach and the Vesdre rivers represent the gauged drained area for the Vesdre reservoir, but this only accounts for 82.3% of the total drained area because 17.7% is ungauged (Figure 4).

*Gauged drained area:* The Helle, Getzbach and Vesdre basins are gauged at three weirs, represented by dots in Figure 3. They constitute the three main tributaries of the dam. The water levels measured at these stations are transformed into discharge using rating curves.

Data from the three aforementioned sources were available. However, it was further necessary to rectify the noise in the data, especially after 2014. For this purpose, a Savitzky-Golay filter (Savitzky & Golay, 1964) was used. The window length of the filter was set to 5 while the polynomial order was 1.

Figure 5 displays the daily statistics (median, percentiles 10-90, 25-75 and maximum) of the inflow discharge across 27 years (1995 - 2022) for the filtered data. The effect of the filter is illustrated in Figure A.2.

*Ungauged drained area:* To account for the ungauged drained area (including the area of the reservoir lake itself), a regionalisation approach was adopted that assumed that the flow rate originating from the ungauged drained area is proportional to the area of the corresponding catchment (Schreider et al., 2002).

Mathematically, this translates to:

$$\begin{aligned} & Q_{in} = Q_{in(\mathrm{H})} + Q_{in(\mathrm{V+G})} + Q_{\mathrm{ungauged}} \\ \Rightarrow\ & Q_{in} = Q_{in(\mathrm{H})} + Q_{in(\mathrm{V+G})} + \frac{A_{\mathrm{ungauged}}}{A_{\mathrm{gauged}}} Q_{in(\mathrm{V+G})} \\ \Rightarrow\ & Q_{in} = Q_{in(\mathrm{H})} + \frac{A_{\mathrm{total}}}{A_{\mathrm{gauged}}} Q_{in(\mathrm{V+G})} \end{aligned} \tag{1}$$

where, V → Vesdre, G → Getzbach and, H → Helle.

### *2.2.2 Reservoir water level*

The prevalent volume of water in the reservoir is determined from the observed reservoir water level with the help of a stage-volume curve (Figure A.3). Table 2 lists operationally significant water levels and the corresponding volumes.

To establish a continuous stage-volume relationship from a discrete set of pairs of stage and volume values, a smooth spline interpolation approach was adopted. The generated spline effectively represents the continuous relationship between stage and volume of the reservoir. This approach was selected for its efficiency in handling the nonlinear nature of the stage-volume relationship especially in intervals where measured data points are sparse and to also ensure continuous derivatives of the curve.

Once again, it was deemed fit to filter the available data using the Savitzky-Golay filter, with window length = 10 and polynomial order = 1 (Savitzky & Golay, 1964). This is because the available data was significantly noisy in certain ranges of the time-series (especially since 01/06/2013). A comparison of the raw and filtered data is presented in Figure 6. For the July 2021 event, it was observed that the filtering process lowers the peak reservoir water level below the MWL. This is because the window length of the filter is not small enough to retain such a sharp gradient. It was verified from the report by Zeimetz et al. (2021) that the water level during the July 2021 event did cross the MWL. Therefore, the raw data was retained specifically for this event. For other events, the filter helps reduce the digital noise without significantly affecting the peak of the water level curve.

#### *2.2.3 Observed releases*

Data pertaining to the release discharge from the reservoir into the Vesdre river was made available by the Service Public de Wallonie (SPW) at an hourly frequency. The discharge was computed using water level sensors and associated rating curves. However, the rating curve and thereby the data was not reliable for all configurations (involving the bottom outlets and the surface spillway) of downstream release. This highlights a major limitation in the monitoring of outflow discharge from the dam.

#### *2.2.4 Water intake by the SWDE*

The primary function of the Eupen reservoir is to supply water to approximately 400,000 residents (Bruwier et al., 2015). The volume of water extracted by the Société Wallonne des Eaux (SWDE) is thus significant. However, from the hourly water intake

(SWDE) data from 1995 to 2022 (provided by SPW) the intake was found to be 0.63 $m^3/s$ which is not of significance to the present analysis catering to flood events.

## ***2.3 Computation of derived variables***

### *2.3.1 Mass balance*

To calculate the outflow discharge from the reservoir, a standard mass balance (Equation 2) was applied. This approach incorporated the time-series data of the inflow discharge $Q_{in}$ into the reservoir (calculated as per Equation 1), along with the series representing the volume of water in the reservoir. The change in the reservoir's volume over a given time interval, $\Delta t$, was equated to the net flow, which is the difference between the inflow and outflow during that same time interval. Hence,

$$Q_{out}(t+\Delta t) = Q_{in}(t+\Delta t) - \frac{V(t+\Delta t) - V(t)}{\Delta t} \tag{2}$$

### *2.3.2 Volume computations*

The outflow volume $V_{out}$, was computed as follows:

$$V_{out} = V_{in}(t) - \left(V(t) - V(t-1)\right) \tag{3}$$

where, $V_{in}$ represents the incoming volume (which is ascertained using inflow discharge) and $V$ represents the extant volume within the reservoir (which is derived from the observed water levels which are converted into volumetric estimates using the reservoir's established volume-height relationship function).

The cumulative volume stored exclusively accounts for the event-specific storage and does not consider pre-event reservoir levels.

### *2.3.3 Rising rates*

To compare the gradients of the rising limbs of the inflow and outflow hydrographs, the rising rate (*R*) for each event hydrograph was calculated as:

$$R = \frac{Q_{\max} - Q_{t_0}}{t_{Q_{\max}} - t_0} \qquad (4)$$

where, $t_0$ is the time corresponding to the start of the event (demarcated manually through visual inspection of hydrographs) and $t_{Q_{\max}}$ is the time corresponding to the peak value of either the inflow or the outflow hydrograph.

### *2.3.4 Flood frequency analysis*

To quantitatively understand the effects of the dam on the characteristics of extreme/moderate flood events, a flood frequency analysis was conducted. The analysis was separately conducted for the inflow and outflow discharges to and from the dam.

The events were chosen using the Annual Maximum Series (AMS) method considering hydrological years from 1995 to 2022. Empirical return period calculations were done based on the formula for Annual Exceedance Probability (AEP):

$$F_i = \frac{(i - \alpha)}{N + 1 - 2\alpha} \qquad (5)$$

where, $F_i$ is the AEP associated with the $i^{th}$ ranked peak (series sorted in descending order of peak discharge), $N$ is the total number of peaks considered and $\alpha$ is a constant ranging between 0 and 1 ($\alpha = 0.4$ adopted in this case, as per Cunnane (1978)).

Several distributions were tried and examined. In the end, a 3-parameter Generalized Extreme Value (GEV) distribution was fitted to the annual maximum series. Care was taken to check consistency of sign of the shape parameter ($\sigma$) of the

GEV distribution to ensure comparability between the GEV fits of the inflow and outflow series (Table 3).

# 3 Results and discussion

In this section the findings of the study have been presented and discussed with sequential focus on various parameters calculated to quantify the effects of the Eupen dam and its operation. An overview of the entire inflow regime has been provided in the form of a hydrological calendar in Figure 8. However, the presentation and discussion of the results concentrate on 18 significant events that occurred in the period spanning from 1995 to 2022. These 18 events were chosen on the basis of the highest peak discharges recorded during the aforementioned period while also being events officially registered as calamities by the Royal Meteorological Institute (RMI) of Belgium.

## *3.1 Inflow*

The hydrological calendar (Figure 8) together with Figure 5 provides insights into the temporal distribution and magnitude of inflow discharges to the reservoir. Both figures indicate that historically floods have occurred throughout the year i.e. there is no clear seasonality in their occurrence. The most severe flood event took place in the summer (July 2021). This highlights the need for a year-round flood management plan. This is reflected in Figure 2 where the normal water level and the maximum water level are horizontal lines with no seasonal variations. This is distinctive feature of this operation protocol, and it does not apply to all dams, not even in the region (Kufeld, 2013). The frequency of occurrence of floods, however, is highest between the months of November and March. In Figure 5, it is also seen that the median inflow in the summer is below the drinking water extraction requirement (0.63 $m^3/s$) which highlights the reason for construction of the dam.

### *3.2 Computed outflow discharge*

Outflow discharge was calculated based on the aforementioned mass balance equation (Equation 2). Figure 9a presents the daily statistics of the computed outflow discharges for each day in the year from 1995 to 2022. In Figure 9b there is an obvious outstanding peak in the month of July. This is attributed to the July 2021 mega-flood (Dewals et al., 2021).

Prior to the July 2021 event, the highest known outflow discharge was 40 $m^3/s$ (23rd January 1995). This value is nearly one-fifth of the peak outflow discharge during the July 2021 event (196 $m^3/s$). The catastrophic nature of the July 2021 mega-event is depicted in the severe impacts it caused, in terms of both material damage and loss of life (Commissariat Spécial à la Reconstruction [CSR], 2022; Dewals et al., 2021).

### *3.3 Comparison of computed and measured outflow*

As per reasons stated in section 2.2.3, the measured outflow values are not always reliable. Nevertheless, a comparison of the computed outflow discharge with those measured is presented herewith.

Figure 10 presents the time-series of discharges for some events for which the measured and computed time-series show moderate/strong agreement, thereby adding credibility to the computations. The comparisons for all other events are presented in Figure A.4.

### *3.4 Comparison of inflow and outflow discharge*

Figure 11 compares the peak of the outflow discharge with the peak of the inflow discharge for all 18 major events. For the majority of the events, the attenuation of the peak was found to be between 50-80%. Overall, the dam was found to attenuate the flood peaks by 9-91%. The 9% value is, in fact, a singular statistical outlier corresponding to the July 2021 flood. Not considering the same yields an average peak attenuation of 61% which is close to the 67% value reported by Graf (2006) and also within the range of 45-70% as reported by Stecher & Herrnegger (2022).

Figure 12 shows the distribution of the considered events over the days in a year. Exactly half of the chosen events occurred during the winter months (late November to March) while the rest are distributed between the summer and autumn months (May to September). The mean peak inflow during the summer months (54 $m^3/s$) is higher than that during the winter months (46 $m^3/s$), even without considering the July 2021 mega-event, which would obviously further skew the mean value in favour of the summer peaks.

Time series data for inflow discharge, outflow discharge, and reservoir water level for the 18 individual events have been presented in Figure A.5 of the appendix. It is apparent that, in none of the considered events, the dam operator proceeded with a substantial pre-release which would have led to a reservoir drawdown prior to the onset of the incoming flood wave (Becker et al., 2022). Figure 13 specifically highlights four of these events. Here, the attenuation of the incoming flood peak can be well observed. In some cases, the outflow hydrograph had no discernible peak at all.

In January 1995 (Figure 13a), the water level prior to the event was above the 358.5 m mark. As per operation rules, if the water level is above this mark during normal operations, then it must be brought back down below this mark via controlled releases while ensuring safety conditions downstream. However, a slightly smaller event (peak inflow discharge = 37 $m^3/s$) took place two weeks prior to this event (Figure A.6). Following that, the water level in the reservoir remained above the 358.5 m mark which meant limited availability of flood storage. The fact that the reservoir level could not be lowered further after the prior event could be due to downstream conditions. Nevertheless, the operators began releasing water almost 16 hours after the inflow hydrograph had begun to rise (corresponding to the peak on 23rd January 1995). This may have been motivated by forecasts, since 3-4 days after this event, slightly smaller events with inflow peaks in the range of 33-37 $m^3/s$ were observed (Figure A.6).

The event of September 2007 (Figure 13b) serves as a typical case for a summer flood. Prior to the event, the release was consistently higher than the inflow. This would explain the low reservoir level as probably due to consumption during the dry season. During the event, the flood volume was utilised to fill up the reservoir. As displayed in Figure A.5, this intent is recurrently observed for most summer floods (1998-09, 2006-05, 2007-08, 2007-09, 2014-07, 2016-05, 2018-05) but also during some winter floods (1999-02, 2004-01, 2015-11). Since, in the case of the September 2007 event, the entire flood volume was accommodated in the reservoir, the outflow hydrograph was almost completely flattened (91% peak reduction). Other summer floods wherein outflow peaks were observed had a mean value of 16 $m^3/s$ (excluding the July 2021 mega-flood).

In March 2019 (Figure 13c), we observe a flood at the tail-end of the winter season. Reservoir water levels were maintained at a high-level in preparation for consumption requirements during the impending dry season. Therefore, the flood storage zone along with a consistent controlled release was utilised to control the flood.

Figure 13d is the case of the July 2021 mega-flood. Consistent with other summer floods, in the build-up to the event, the operators maintain a very low release (< 1 $m^3/s$) with the goal of filling up the reservoir. However, an unprecedented intensity and amount of rainfall (Journée et al., 2023) led to a staggeringly high inflow peak (Table A.7) and the reservoir was filled, in a matter of hours. The reservoir level crossed the MWL mark around 22:00 on 14-07-2021 and then the 361 m mark at 01:00 on 15-07-2021, which has been stated by Zeimetz et al. (2021) to be the “maximum lake height to guarantee structural safety of the structure”. This led to the downstream release of 196 $m^3/s$.

Figure 14 shows the ratio of the attenuation of the outflow peak with respect to the inflow peak (hereafter, peak attenuation ratio) against the ratio of the cumulative (incoming) flood volume to the available volume in the reservoir at the onset of the event (hereafter, volume ratio). The vertical dotted line at volume ratio equal to 1 separates the flood events into two categories - those for which the flood volume, in principle, could be completely accommodated in the reservoir (points on the left of the line) and those which would require downstream release (points on the right of the line). Accordingly, we find that out of the 9 events that have a volume ratio less than one, 7 are summer floods, which is consistent with the fact that reservoir water levels are relatively low during this season. Winter floods, especially those in January and February, predominantly had volume ratios greater than 1 owing to the transition towards higher reservoir water levels as per the operational rules (Figure 2). The case of February 2022, a winter flood, having a very low volume ratio is to be attributed more to the low reservoir water level than a low peak inflow (which was 40 $m^3/s$, Figure A.5(r)).

In Figure 14, for lower ranges of volume ratio, we find that for similar volume ratios, a range of peak attenuation ratios may be achieved based on how the dam is operated. This may again be linked with the fact that, when the incoming flood volume can be mostly or completely accommodated by the dam, there is room for variability on the dam operator's part as to how much water is to be retained (for drinking water supply) and how much is to be released (to maintain flood control capacity for the future).

For higher volume ratios, it is seen that significant peak reduction was not achieved unless the release began with, or very shortly after, the arrival of the incoming flood wave. For instance, the floods of March 2019 had the highest volume ratio of all cases considered (even July 2021) and yet, the peak was reduced by almost 60%. This is because a significant downstream release began immediately with the incoming flood wave. In doing so, the operators were able to reserve the flood storage zone for the arrival of the main peak (Figure 13c). Such a release, beginning close to the arrival of the incoming flood wave, was not carried out in the cases of 2021-01, 1995-01 and 2021-07. Specifically, in the case of the July 2021 mega-flood, it is observed that significant release did not begin until the water level approached the maximum water level. Once the water level rose beyond the maximum water level, a large release with a sharp gradient became inevitable in order to avoid jeopardizing the dam's structural integrity. This implied a very small peak attenuation of only 8%. It is worth considering that the consequences of such a flood during winter could potentially be worse given the high reservoir water levels maintained during those months (Figure 7).

In the absence of forecast data, based on which dam operations are conducted, it is difficult to further interpret such cases. Nevertheless, the analysis reveals that attenuation of incoming flood peaks is largely contingent on dam operations undertaken after a forecast is received and also on the prevalent conditions of the dam due to the seasonal nature of the management plan.

### *3.5 Comparison of time-to-peak of inflow and outflow discharge*

In Figure 15, a comparison is made between the time to peak of the inflow and outflow discharge from the start of each event. In all but two cases (1998-09 and 2006-05), the outflow discharge's time to peak is more than that of the inflow discharge. In the present study, the delay spans from 0 to 68 hours.

Most events have a peak delay time greater than or equal to zero, meaning the peak outflow occurs at the same time or after the peak inflow. This delay in peak outflow reflects the dam's storage and delay effect on the inflowing water. However, two events show a peak delay less than zero, suggesting instances where the peak outflow precedes the peak inflow. These instances correspond to the events of 1998-09 and 2006-05, where one observes minor releases (< 14 $m^3/s$). In both cases, the incoming flood volume was almost entirely accommodated in the reservoir, indicating that the releases were perhaps more precautionary than necessary.

Figure 16 provides further insight into what governs the peak delay. The plot of the relative peak delay against the volume ratio (as defined in the previous section) reveals a significant direct correlation between the two i.e., relative peak delay is higher for a higher volume ratio. This relation however does not hold when both, the volume ratio, and the peak inflow, are significantly high - which is the case of all the three outliers. The fact that simultaneous occurrence of both is important, is substantiated by the observation that there are events with low volume ratio but high peak inflow (and vice versa) which still obey the trendline. For e.g., the event of 2021-01 has a higher volume ratio than that of 2019-03 (outlier) but has a relatively lower peak inflow discharge.

### *3.6 Comparison between maximum gradient for outflow and inflow discharge*

Figure 17 presents a comparison between the rising rates of inflow and outflow discharge.

The data exhibits a clustering of points at the lower end of the gradient scale, with a notable outlier at the higher end. This suggests that for most observed events, the rising rate - both in and out of the dam - is relatively moderate. The outlier, which corresponds to the event of July 2021, indicates a significantly higher gradient. The plot also indicates that the dam's outflow does not rise as steeply as the inflow for all events, reflected in the points lying below the line of equality. This is a direct result of the dam's operation, which temporally spreads the outflow hydrograph.

The July 2021 outlier, with an inflow gradient above 175 $m^3/s^2$ and an outflow gradient correspondingly high, shows how the dam released water at a much faster rate, knowingly due to safety protocols in response to a large inflow volume. Notably, across all events, the outflow hydrograph rising rates are reduced by 8-91% with respect to that of the inflow hydrograph. The mean percentage reduction of the rising rate was found to be 61% which is in good agreement with the value of 60% and 58% as reported by Graf (2006) and Fantin-Cruz et al. (2015) respectively.

### *3.7 Comparison between cumulative inflow and outflow volume*

This section details the storage effect of the dam by comparing the total volume of water that flows into the dam and that which flows out, for each of the major events.

Again, in the absence of the dam, the outflow volume would be equal to the inflow volume (i.e., natural outflow volume). The presence of it was found to reduce the outflow volumes by 2% to 94%. The median flood volume reduction was 44% which is comparable to the 30% value reported by Brunner (2021). The interquartile ranges are close to 60% for both the present study (15-75%) and the study of Brunner (2021) (3-64%). Figure 18 compares the cumulative volume that flows into the reservoir and the cumulative volume that flows out of the reservoir from the beginning of the event for each major event. It can be noticed that for one event, the cumulative outflow volume is 28% greater than the cumulative inflow volume. This event corresponds to the one of

January 1995 (Figure 19a) where the downstream release was maintained between 20-30 m$^3$/s even after the inflow peak to create additional storage in the reservoir.

Once again, however, the July 2021 event stands out with a cumulative inflow volume almost twice the average for all other events. More significantly, the cumulative outflow volume for this mega-flood was 2.88 times the average of all the other major events.

Figure 19 details the cumulative volumetric data for four of the events. This comprises the volumes entering and exiting the reservoir, as well as the volume thereby retained within the reservoir (storage). The difference between the beginning and the end of the storage curve represents the net storage attributable to the particular event.

Figure 19a presents a high initial volume in the reservoir owing to the fact that it was a winter event. The possible reasons for this initial volume being above the NWL threshold are discussed in Section 3.4. A drawdown below the NWL threshold is also observed after the recession of the flood.

In Figure 19b, the cumulative outflow volume is very small since the inflow volume is almost entirely used to fill the reservoir.

Figure 19c (November 2015) and Figure 19d (July 2021) present two cases with particularly high cumulative inflow volumes. The initial volume is lower in the former case than the latter. The two cases differ in terms of gradient of the cumulative inflow volume curve, which is much higher in the case of the July 2021 flood. This is a direct consequence of the peak discharge – highlighting the fact that the peak flow is more critical than the volume of the flood (which may be well distributed over a period of time).

### *3.8 Flood frequency analysis*

Figure 20 presents the GEV fit for both the inflow and outflow timeseries. It is observed that the dam significantly reduces the discharges associated with varying return periods. It has also been shown in Figure A.8 that uncertainties associated with high return period floods are significantly large.

Table 4 lists all the events identified as per the AMS methodology, the associated peak discharges and return periods, for both the inflow and outflow. Those corresponding to the events considered in the study have been highlighted. Four inflow events, viz. 1998-09, 2007-08, 2014-07, 2016-06 and 2018-06, were no longer an event (in the outflow series) due to the dam operation's peak attenuation effects. For several inflow events, the return periods changed in the outflow series. The return periods in the outflow series for 2004-01, 2006-05, 2011-01 and 2019-03 are lower than the corresponding return periods in the inflow series. On the other hand, the opposite is true for the events of 1995-01 and 2000-09. It is to be noted that not all the 18 events primarily investigated in this study feature in Table 4. This is because the AMS looks at the annual maxima of inflow and outflow in a given hydrological year, whereas the 18 events had an additional criterion of being reported as calamities by RMI.

Figure 21, on the other hand, shows the relative reduction of discharges corresponding to floods of different annual exceedance probabilities because of the dam. Several return periods from 5 to 1000 years were chosen and the corresponding $Q_{in}$ and $Q_{out}$ values were derived from the GEV fits in Figure 20. The relative reduction is calculated as $( Q_{in} – Q_{out} ) / Q_{in}$. Figure 21 indicates that the dam reduces the magnitude of floods of different return periods by 38-51%. This corresponds well with the values reported by Mei et al. (2017). Specifically, they reported that for dams which are only partly responsible for flood control (as in the present case), a 40% decrease in flood magnitudes is observed. This, again, is within the presently computed range.

## 4 Conclusion

This research focused on quantifying the Eupen dam's impact on the Vesdre river's flow rate. The total inflow and outflow discharges were compared for 18 moderate/extreme flood events. The key findings were:

(1) The dam reduced the peak discharge by 9 to 91 %.

(2) For certain flood events, the dam flattened out the peaks (no peak in the outflow).

(3) The dam delayed the peak discharge by 0 to 68 hours.

(4) The dam decreased the outflowing flood volume by 2 to 94 %.

(5) The dam slowed the rising rate in the outflow hydrograph by 1.09 to 11.16 times with respect to that of the inflow hydrograph.

(6) From the perspective of an extreme value analysis, the dam reduced the floods of return periods ranging from 5 to 1000 years by a factor of 1.6 to 2.

The broad range of values for the above features are a result of the seasonal nature of the operational guidelines as well as human discretion linked with the operation of the dam, which often results in different outflow hydrographs from relatively similar incoming floods and reservoir levels. Other aspects also contribute to explain the variability in the results, such as the fact that for certain flood events the storage capacity of the dam renders the outflow hydrographs almost flat with no obvious peak (Figures A.5b, A.5f, A.5h and A.5j). In such cases, the outflow hydrograph carries very little of the signature of the inflow hydrograph, making it difficult to identify a coherent and obvious peak and therefore also its timing. For 14 events (out of the 18 considered here) the inflow peaks were reduced to under 30 $m^3$/s. Eleven of those 14 inflow peaks were attenuated to below 22 $m^3$/s. How useful these peak attenuations are with regards to downstream flooding depends on the conditions elsewhere in the catchment.

Further, a significant direct correlation was found between the relative peak delay and the volume ratio. It was simultaneously noted that this relation did not hold when both the volume ratio and the peak inflow discharge were significantly high (leading to a low relative peak delay).

Also, notably, reconstructed flow data for the July 2021 mega-flood were made part of the analysed time-series. The analysis revealed that the dam, in its antecedent condition, provides scant benefits during such a mega-event (as compared to formerly observed extreme flood events).

To the best of the authors' knowledge, this is one of the few studies that considers reservoir level data, not only in its computations but also in the interpretation of different dam operations undertaken and their outcomes. A future perspective would therefore be to carry out similar studies with a larger sample size and with information about reservoir conditions included in the discussions.

In meticulously analysing 18 critical events, the present study offers insights into flood-control capabilities of a multi-purpose dam. The present work informs future studies that aim at development of more robust operational plans capable of better handling such events at different times of the year. The variability in the dam's impact based on operational discretion also highlights the need for more standardized guidelines for dam operation during flood events. This is all the more critical in light of the increasing frequency of extreme weather events due to climate change. In this regard, the analysis presented in this study helps identify variables and conditions that could inform the design of such extreme-event scenario studies in the future.

Nevertheless, these findings are subject to uncertainties, including equipment-related uncertainties and uncertainties from the base data. The fact that the outflow discharge is not known from the field is a key limitation. Further, although widespread, the use of regionalisation techniques to estimate the contribution of ungauged basin introduces uncertainties into the computed inflow discharge (Tara & Paulin, 2013). Future research could therefore also focus on developing a hydrological model to compute the total inflow discharge from precipitation and temperature data, thereby gauging the uncertainty linked to the drained ungauged sub-basin.

## 5 Acknowledgements

The Authors gratefully acknowledge the insightful comments received from Dr. Bernhard Becker as well as from an anonymous Reviewer  and the Editor. They have enabled a substantial improvement of the contents of the paper.

## References

Assani, A. A., Stichelbout, É., Roy, A. G., & Petit, F. (2006). Comparison of impacts of dams on the annual maximum flow characteristics in three regulated hydrologic regimes in Québec (Canada). *Hydrological Processes*, *20*(16), 3485–3501. https://doi.org/https://doi.org/10.1002/hyp.6150

Ayalew, T. B., Krajewski, W. F., & Mantilla, R. (2013). Exploring the effect of reservoir storage on peak discharge frequency. *Journal of Hydrologic Engineering*, *18*(12), 1697–1708.

Baker, D. B., Richards, R. P., Loftus, T. T., & Kramer, J. W. (2004). A new flashiness index: Characteristics and applications to midwestern rivers and streams. *JAWRA Journal of the American Water Resources Association*, *40*(2), 503–522. https://doi.org/https://doi.org/10.1111/j.1752-1688.2004.tb01046.x

Batalla, R. J., Gómez, C. M., & Kondolf, G. M. (2004). Reservoir-induced hydrological changes in the Ebro River basin (NE Spain). *Journal of Hydrology*, *290*(1), 117–136. https://doi.org/https://doi.org/10.1016/j.jhydrol.2003.12.002

Becker, B., Kim, J., & Pummer, E. (2022, September 12). Methods for addressing uncertainty in reservoir operations under flood conditions. *Hydropower Scheduling Conference*. https://www.sintef.no/contentassets/106baff79dc44ca5897fea4c51b1cfa7/p4_4-becker_deltares.pdf

Becker, B., Ochterbeck, D., & Piovesan, T. (2023). A comparison of the homotopy method with linearisation approaches for a non-linear optimization problem of operations in a reservoir cascade. *Energy Systems*. https://doi.org/10.1007/s12667-023-00608-w

Brunner, M. I. (2021). Reservoir regulation affects droughts and floods at local and regional scales. *Environmental Research Letters*, *16*(12). https://doi.org/10.1088/1748-9326/ac36f6

Bruwier, M., Erpicum, S., Pirotton, M., Archambeau, P., & Dewals, B. J. (2015). Assessing the operation rules of a reservoir system based on a detailed modelling chain. *Natural Hazards and Earth System Sciences*, *15*(3), 365–379. https://doi.org/10.5194/nhess-15-365-2015

Commissariat Spécial à la Reconstruction [CSR]. (2022). *1 an après les inondations … Bilan de la gestion post-inondations et continuité de la reconstruction*. https://www.wallonie.be/sites/default/files/2022-07/Bilan%20complet%20CSR%2026%20juillet%202022.pdf

Cunnane, C. (1978). Unbiased plotting positions — A review. *Journal of Hydrology*, *37*(3), 205–222. https://doi.org/https://doi.org/10.1016/0022-1694(78)90017-3

Cuvelier, T., Archambeau, P., Dewals, B., & Louveaux, Q. (2018). Comparison Between Robust and Stochastic Optimisation for Long-term Reservoir Management Under Uncertainty. *Water Resources Management*, *32*(5), 1599–1614. https://doi.org/10.1007/s11269-017-1893-1

Dewals, B., Erpicum, S., Pirotton, M., & Archambeau, P. (2021). July 2021 extreme floods in the Belgian part of the Meuse basin. *Hydrolink*, *4*, 104–107. https://www.iahr.org/library/hydrolink?hid=412

Ely, P., Fantin-Cruz, I., Tritico, H., Girard, P., & Kaplan, D. (2020). Dam-Induced Hydrologic Alterations in the Rivers Feeding the Pantanal. *Frontiers in Environmental Science*, *8*, 579031. https://doi.org/10.3389/fenvs.2020.579031

Fantin-Cruz, I., Pedrollo, O., Girard, P., Zeilhofer, P., & Hamilton, S. K. (2015). Effects of a diversion hydropower facility on the hydrological regime of the Correntes

River, a tributary to the Pantanal floodplain, Brazil. *Journal of Hydrology*, *531*, 810–820. https://doi.org/10.1016/j.jhydrol.2015.10.045

Graf, W. (2006). Downstream hydrologic and geomorphic effects of large dams on American rivers. *Geomorphology*, *79*(3–4), 336–360. https://doi.org/10.1016/j.geomorph.2006.06.022

Gutenson, J. L., Tavakoly, A. A., Wahl, M. D., & Follum, M. L. (2020). Comparison of generalized non-data-driven lake and reservoir routing models for global-scale hydrologic forecasting of reservoir outflow at diurnal time steps. *Hydrol. Earth Syst. Sci.*, *24*(5), 2711–2729. https://doi.org/10.5194/hess-24-2711-2020

ICOLD. (1994). *Technical dictionary on dams*.

Jordan, F. M., Boillat, J.-L., & Schleiss, A. J. (2012). Optimization of the flood protection effect of a hydropower multi-reservoir system. *International Journal of River Basin Management*, *10*(1), 65–72. https://doi.org/10.1080/15715124.2011.650868

Journée, M., Goudenhoofdt, E., Vannitsem, S., & Delobbe, L. (2023). Quantitative rainfall analysis of the  2021 mid-July flood event in Belgium. *Hydrol. Earth Syst. Sci.*, *27*(17), 3169–3189. https://doi.org/10.5194/hess-27-3169-2023

Kufeld, M. (2013). *Adaption of reservoir operation to climate change : evaluation of performance and robustness* [Doctoral dissertation, RWTH Aachen]. https://publications.rwth-aachen.de/record/229467

Lehner, B., Liermann, C. R., Revenga, C., Vörösmarty, C., Fekete, B., Crouzet, P., Döll, P., Endejan, M., Frenken, K., Magome, J., Nilsson, C., Robertson, J. C., Rödel, R., Sindorf, N., & Wisser, D. (2011). High-resolution mapping of the world's reservoirs and dams for sustainable river-flow management. *Frontiers in Ecology* *and the Environment*, *9*(9), 494–502. https://doi.org/https://doi.org/10.1890/100125

Mailhot, A., Talbot, G., Ricard, S., Turcotte, R., & Guinard, K. (2018). Assessing the potential impacts of dam operation on daily flow at ungauged river reaches. *Journal of Hydrology: Regional Studies*, *18*, 156–167. https://doi.org/10.1016/j.ejrh.2018.06.006

Mei, X., Gelder, P. H. A. J. M. Van, Dai, Z., & Tang, Z. (2017). Impact of dams on flood occurrence of selected rivers in the United States. *Frontiers of Earth Science*, *11*(2), 268–282. https://doi.org/10.1007/s11707-016-0592-1

Ministère des Travaux Publics, Administration des voies hydrauliques, & Service des Barrages. (1986). *Les Barrages Belges*.

Rahman, S., & Bowling, L. (2019). Streamflow Impacts of Management and Environmental Change in the Upper Wabash River Basin. *Journal of Hydrologic Engineering*, *24*(3). https://doi.org/10.1061/(asce)he.1943-5584.0001750

Richter, B. D., Baumgartner, J. V, Powell, J., & Braun, D. P. (1996). A Method for Assessing Hydrologic Alteration within Ecosystems. *Conservation Biology*, *10*(4), 1163–1174. https://doi.org/https://doi.org/10.1046/j.1523-1739.1996.10041163.x

Savitzky, A., & Golay, M. J. E. (1964). Smoothing and Differentiation of Data by Simplified Least Squares Procedures. *Analytical Chemistry*, *36*(8), 1627–1639. https://doi.org/10.1021/ac60214a047

Schreider, S. Y., Jakeman, A. J., Gallant, J., & Merritt, W. S. (2002). Prediction of monthly discharge in ungauged catchments under agricultural land use in the Upper Ping basin, northern Thailand. *Mathematics and Computers in Simulation*, *59*(1), 19–33. https://doi.org/https://doi.org/10.1016/S0378-4754(01)00390-1

Song, X., Zhuang, Y., Wang, X., Li, E., Zhang, Y., Lu, X., Yang, J., & Liu, X. (2020). Analysis of Hydrologic Regime Changes Caused by Dams in China. *Journal of Hydrologic Engineering*, *25*(4), 5020003. https://doi.org/10.1061/(ASCE)HE.1943-5584.0001891

Stecher, G., & Herrnegger, M. (2022). Impact of hydropower reservoirs on floods: evidence from large river basins in Austria. *Hydrological Sciences Journal*, *67*(14), 2082–2099. https://doi.org/10.1080/02626667.2022.2130332

Tara, R., & Paulin, C. (2013). Streamflow Prediction in Ungauged Basins: Review of Regionalization Methods. *Journal of Hydrologic Engineering*, *18*(8), 958–975. https://doi.org/10.1061/(ASCE)HE.1943-5584.0000690

Terrier, M., Perrin, C., de Lavenne, A., Andréassian, V., Lerat, J., & Vaze, J. (2021). Streamflow naturalization methods: a review. *Hydrological Sciences Journal*, *66*(1), 12–36. https://doi.org/10.1080/02626667.2020.1839080

Yun, X., Tang, Q., Wang, J., Liu, X., Zhang, Y., Lu, H., Wang, Y., Zhang, L., & Chen, D. (2020). Impacts of climate change and reservoir operation on streamflow and flood characteristics in the Lancang-Mekong River Basin. *Journal of Hydrology*, *590*. https://doi.org/10.1016/j.jhydrol.2020.125472

Zeimetz, F., Launay, M., Bourqui, P., Calixte, E., Fallon, C., & Teller, J. (2021). *Analyse indépendante sur la gestion des voies hydrauliques lors des intempéries de la semaine du 12 juillet 2021 (Belgique)* (Issue Lot1).

Table 1: Summary of studies on dam impacts on streamflow and flood characteristics (✓ - considered, × - not considered).

| Reference | No. of cases | Peak reduction | Peak delay | Flood volume | Discharge gradient | FFA | Reservoir level data (input) | Remarks |
|---|---|---|---|---|---|---|---|---|
| Graf (2006) | 36 | ✓ | ✓ | × | ✓ | × | × | Use of Indicators of Hydrologic Alteration (IHA) |
| Ayalew et al. (2013) | 1 | ✓ | × | × | × | ✓ | ✓ | Effects of active and passive dam regulation |
| Fantin-Cruz et al. (2015) | 1 | ✓ | ✓ | × | ✓ | × | ✓ | Use of Indicators of Hydrologic Alteration (IHA) |
| Mei et al. (2017) | 38 | ✓ | × | × | × | ✓ | × | Comparison of annual averaged statistics |
| Mailhot et al. (2018) | 4,200 | × | × | × | × | × | × | Degree of regulation (DOR) used to isolate the impact of dam operation |
| Rahman & Bowling (2019) | 6 | ✓ | × | × | ✓ | × | × | Annual as well as some event-based statistics reported |
| Yun et al. (2020) | 6 | ✓ | × | × | × | ✓ | × | Report relative changes for flood events |
| Brunner (2021) | 114 | ✓ | × | ✓ | × | × | × | Report relative change incurred by reservoir influence; also considers droughts |
| Stecher & Herrnegger (2022) | 8 | ✓ | × | × | × | ✓ | × | Annual as well as some event-based statistics reported |

Table 2: Operationally significant reservoir water levels and corresponding volumes

| **Reservoir water level (m TAW)** | **Volume ($Mm^3$)** | **Remarks** |
|---|---|---|
| 360.8 | 24 | Maximum water level |
| 358.5 | 21 | Normal water level |
| 342.5 to 355.5 | 7.7 to 18 | Season-dependent value of reservoir water level under which only drinking water supply and minimal d/s release is allowed |
| 308.18 | $8 \times 10^{-3}$ | Dead storage |

Table 3: Parameters of the GEV distribution.

| **AMS** | **Location parameter ($\mu$)** | **Scale parameter ($\sigma$)** | **Shape parameter ($\xi$)** |
|---|---|---|---|
| Inflow | 0.648 | 0.704 | -0.854 |
| Outflow | 0.792 | 0.694 | -0.472 |

Table 4: Annual maxima series for $Q_{in}$ and $Q_{out}$ with their corresponding return periods (sorted in increasing order of return periods).

| Date | $Q_{in}$ | $T_{in}$ |
|---|---|---|
| 1997-02 | 24.64 | 1.02 |
| 2019-11 | 24.78 | 1.06 |
| 2010-02 | 27.26 | 1.11 |
| 2001-04 | 27.63 | 1.15 |
| 2017-03 | 28.34 | 1.20 |
| 2007-12 | 30.23 | 1.26 |
| 2009-02 | 31.58 | 1.32 |
| 1996-08 | 32.05 | 1.39 |
| 2012-12 | 32.95 | 1.46 |
| 2002-12 | 33.19 | 1.55 |
| 2015-01 | 35.68 | 1.64 |
| 2012-01 | 36.69 | 1.74 |
| 2004-11 | 41.34 | 1.86 |
| 2018-06 | 44.39 | 2.00 |
| 2004-01 | 44.55 | 2.16 |
| 2006-05 | 45.48 | 2.34 |
| 2002-02 | 46.10 | 2.57 |
| 1995-01 | 48.21 | 2.83 |
| 2016-06 | 49.57 | 3.16 |
| 2000-09 | 50.50 | 3.58 |
| 1999-03 | 52.12 | 4.12 |
| 2019-03 | 52.25 | 4.86 |
| 2014-07 | 56.08 | 5.91 |
| 1998-09 | 57.69 | 7.56 |
| 2011-01 | 67.14 | 10.46 |
| 2007-08 | 70.70 | 17.00 |
| 2021-07 | 215.28 | 45.33 |

| Date | $Q_{out}$ | $T_{out}$ |
|---|---|---|
| 1995-11 | 5.39 | 1.02 |
| 2004-01 | 10.75 | 1.06 |
| 1996-12 | 11.63 | 1.11 |
| 2005-02 | 11.67 | 1.15 |
| 2006-05 | 13.79 | 1.20 |
| 2007-02 | 14.79 | 1.26 |
| 2013-07 | 14.99 | 1.32 |
| 2003-01 | 15.03 | 1.39 |
| 2009-03 | 15.16 | 1.46 |
| 1998-03 | 15.46 | 1.55 |
| 2016-02 | 17.19 | 1.64 |
| 2010-02 | 17.31 | 1.74 |
| 2018-01 | 18.94 | 1.86 |
| 2001-04 | 19.71 | 2.00 |
| 2017-03 | 20.66 | 2.16 |
| 2012-01 | 22.51 | 2.34 |
| 2019-03 | 23.70 | 2.57 |
| 2007-12 | 26.08 | 2.83 |
| 2011-01 | 27.06 | 3.16 |
| 2020-03 | 27.44 | 3.58 |
| 2015-03 | 30.14 | 4.12 |
| 2000-09 | 31.91 | 4.86 |
| 1999-03 | 32.22 | 5.91 |
| 2002-02 | 34.39 | 7.56 |
| 2014-06 | 38.24 | 10.46 |
| 1995-01 | 40.37 | 17.00 |
| 2021-07 | 196.61 | 45.33 |

Figure 1: The Vesdre reservoir (Cuvelier et al., 2018).

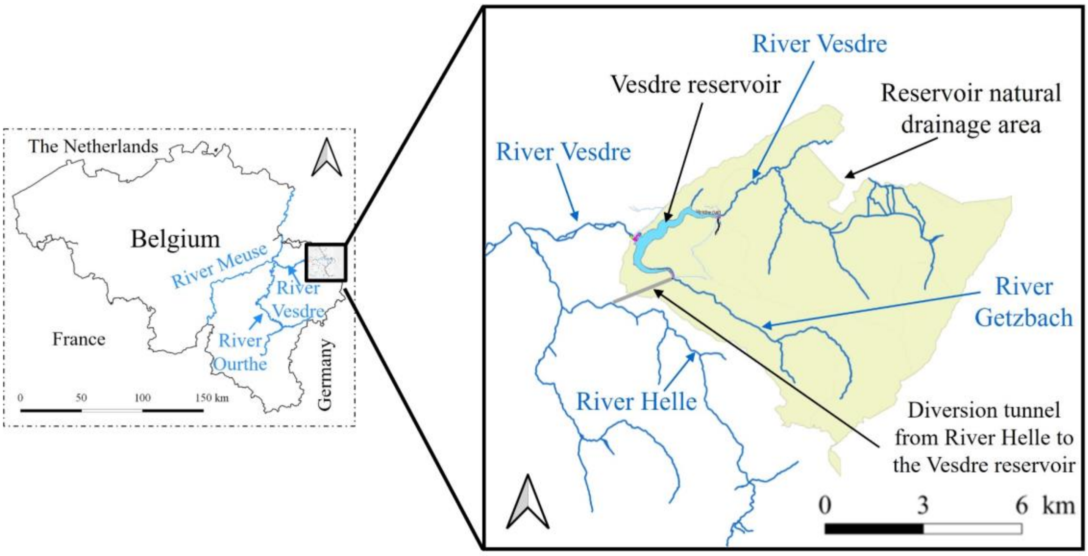


Figure 2: Operational guidelines of the Eupen dam (based on Zeimetz et al. (2021)).

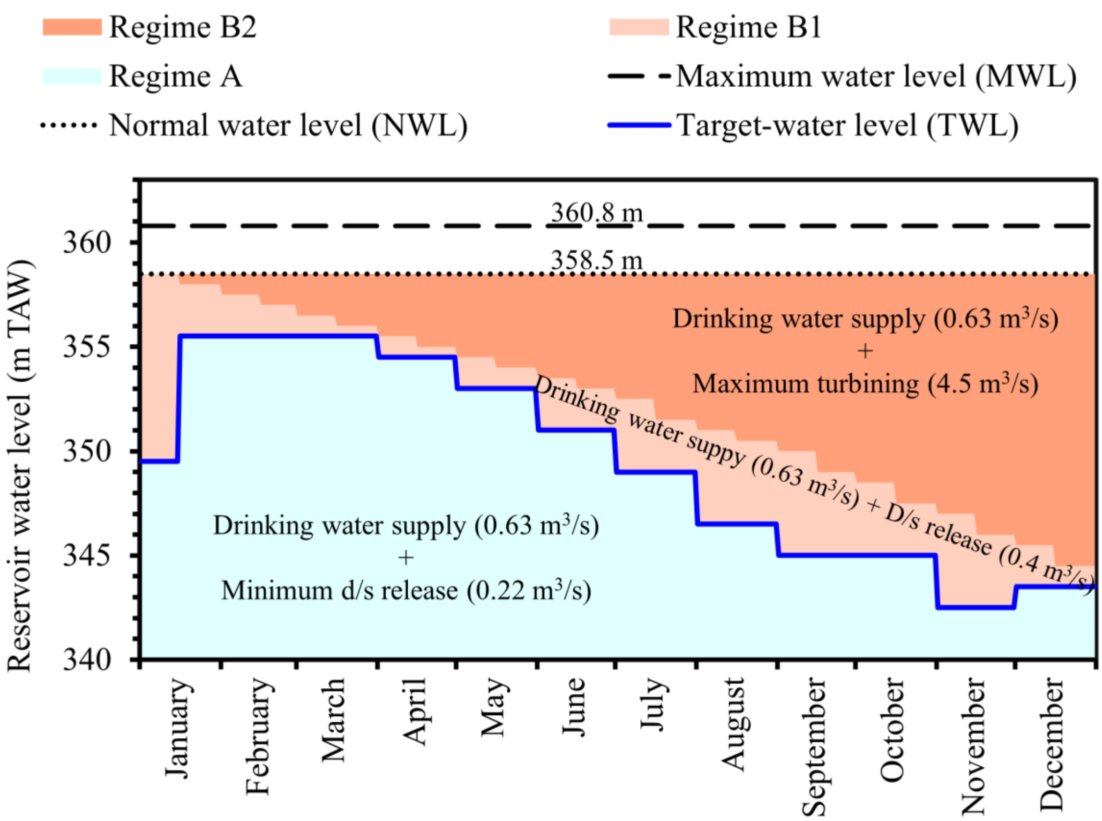

Figure 3: Schematic layout of the Vesdre reservoir. The blue dots correspond to the measuring stations from which time series are available.

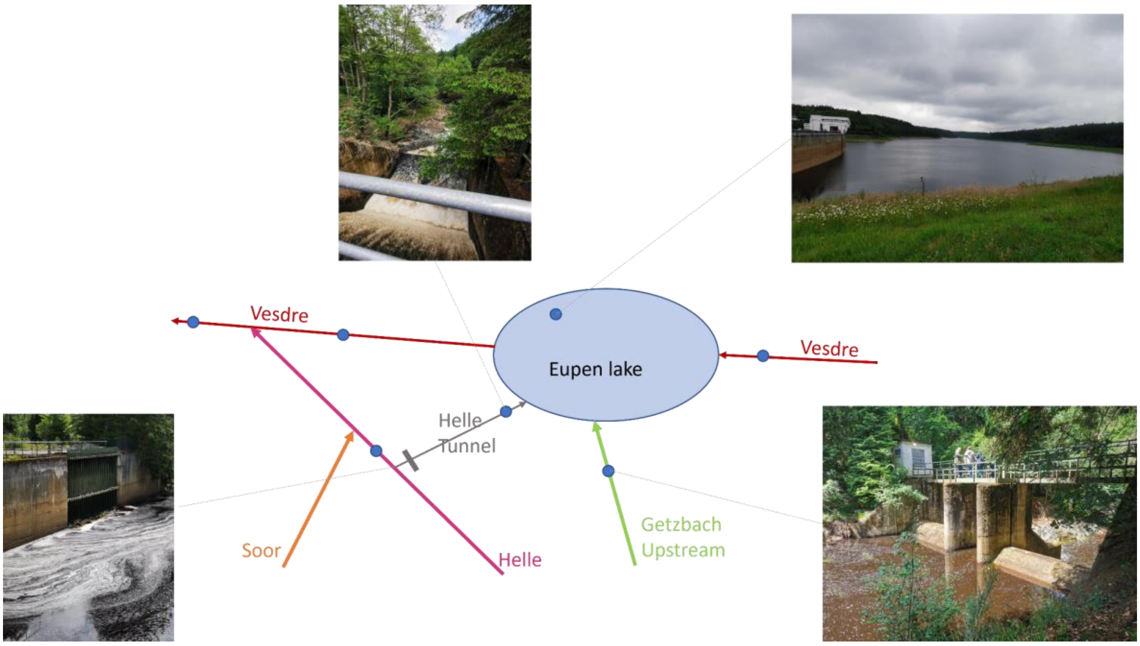


Figure 4: Percentage share of drained catchment areas (including the gauged and ungauged components).

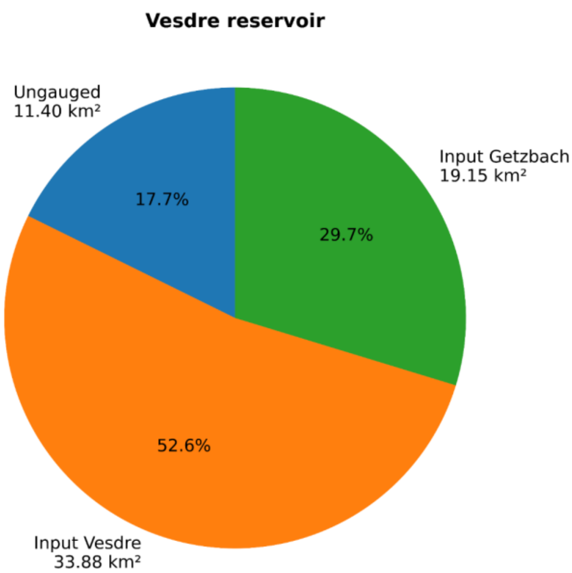

Figure 5: Inflow over the days in a year as median, max and variation computed for the period from 1995 to 2022.

(a) Median, percentiles and drinking water demand

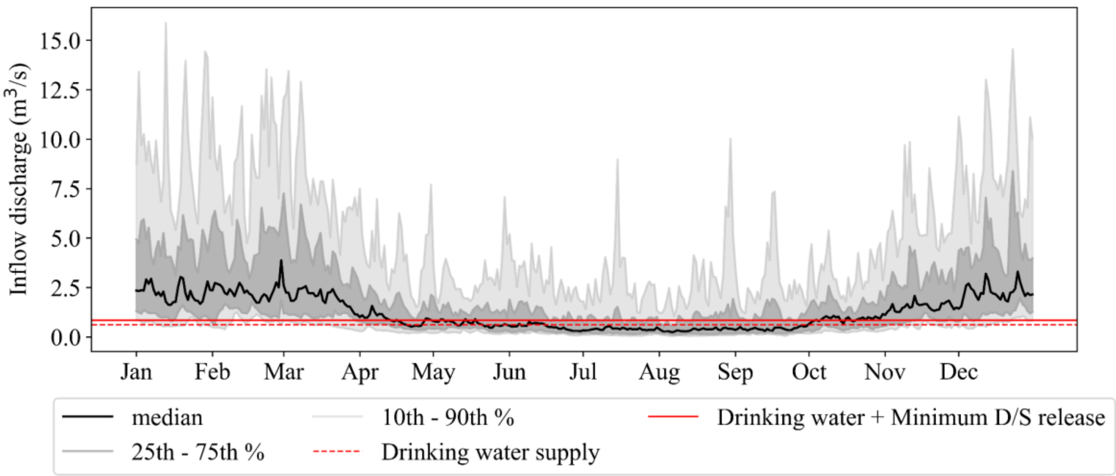


(b) Maximum inflow discharge

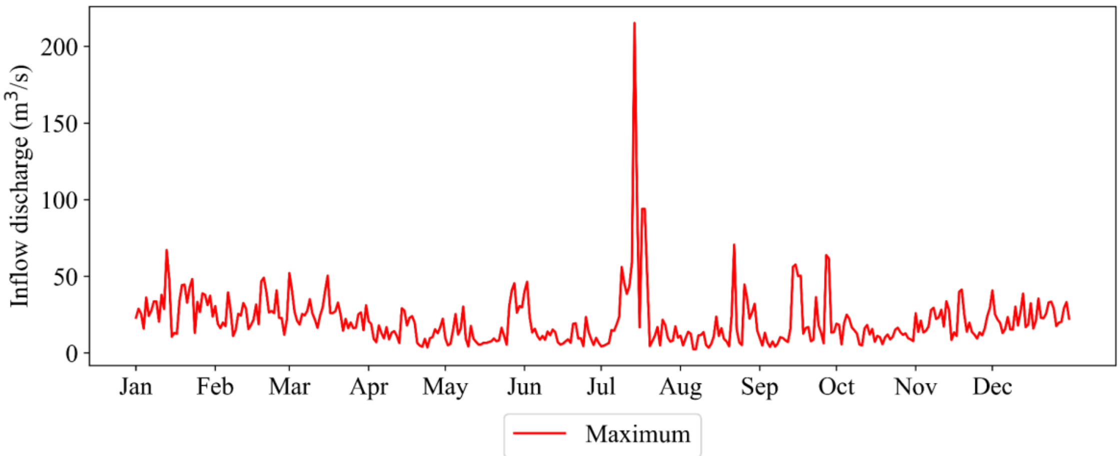

Figure 6: Comparison of raw and filtered reservoir water level data.

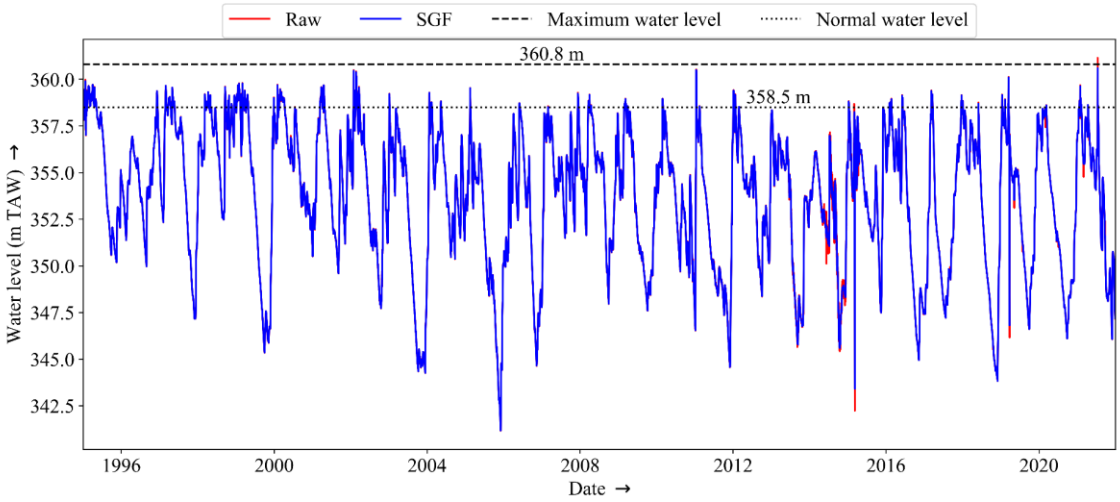


Figure 7: Median, maximum, and minimum reservoir water level over the days in the year from 1995 to 2022.

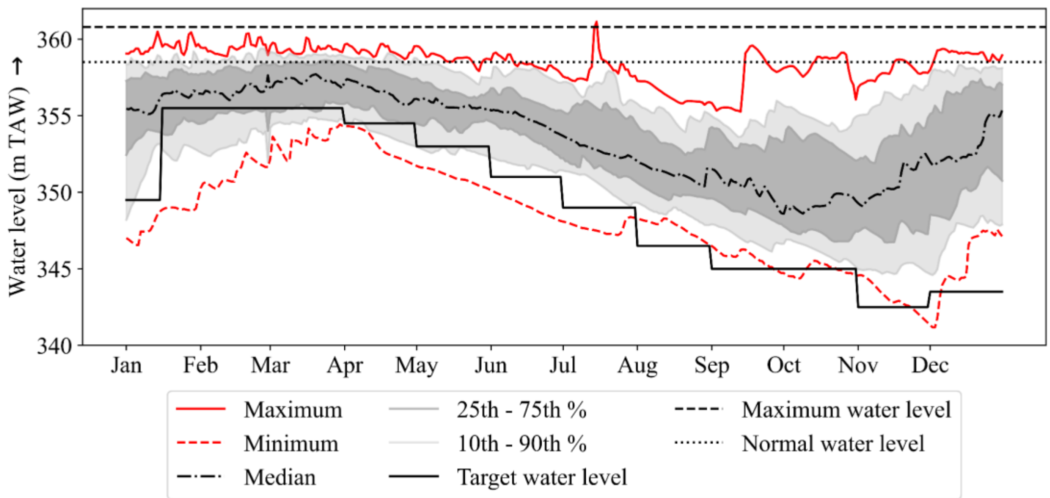

Figure 8: Hydrological calendar. (Note: 29/02 for all non-leap years and post 4th May 2022, the data is depicted in black implying ‘no data’)

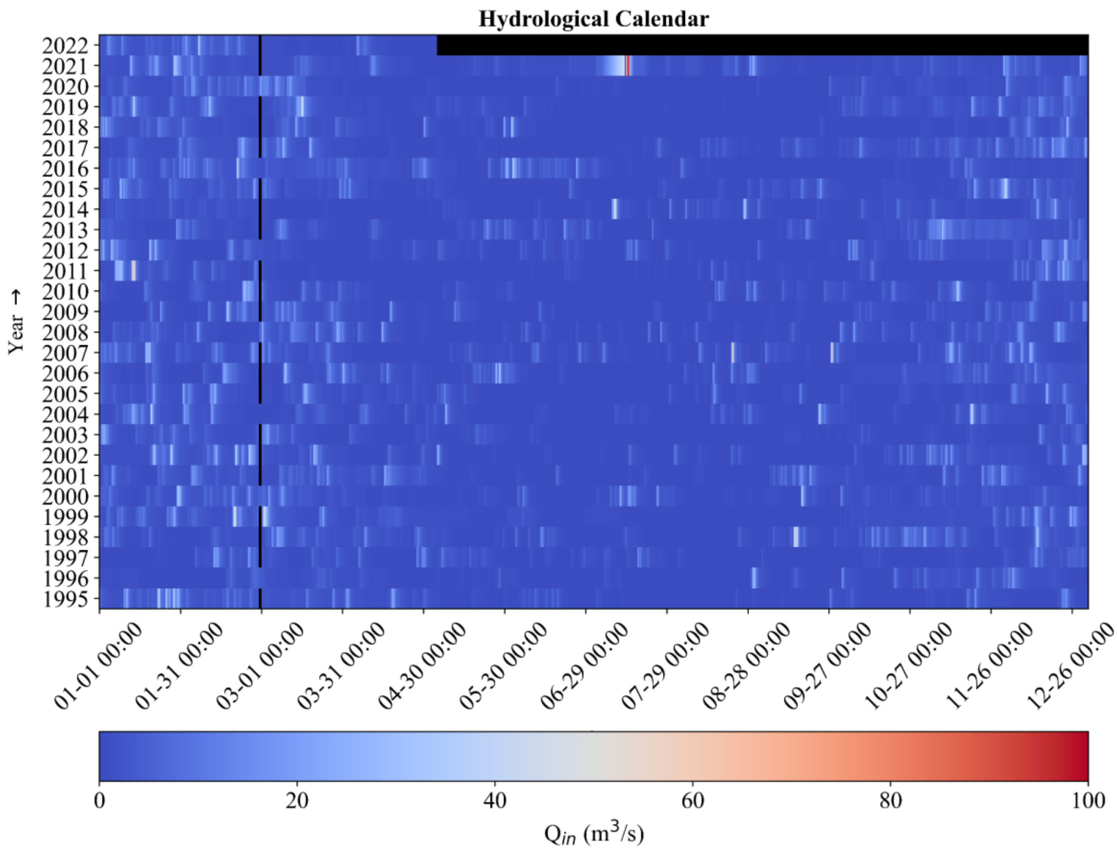

Figure 9: Computed outflow over the days in a year as (above) median, percentiles and (below) maximum.

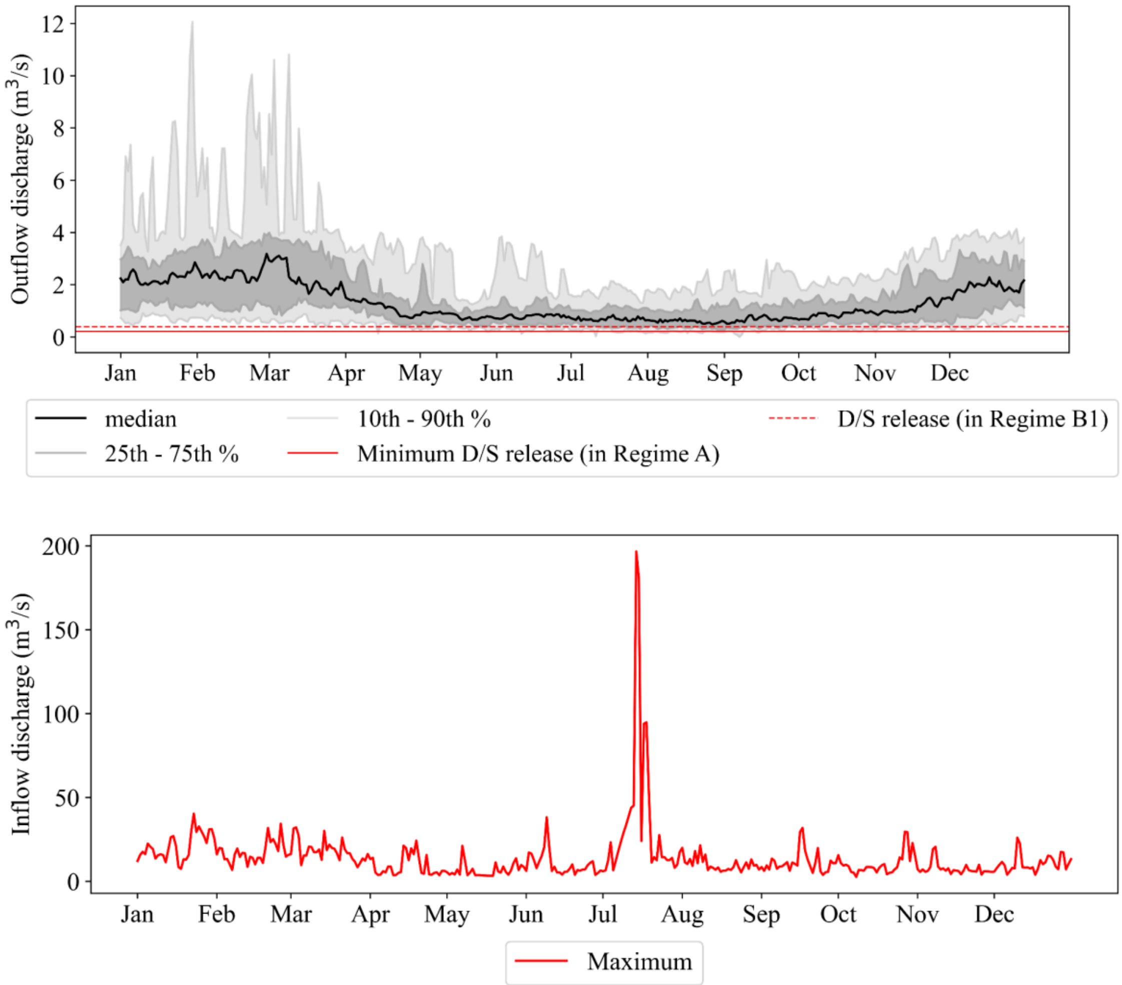

Figure 10: Comparison of measured and computed outflow discharge.

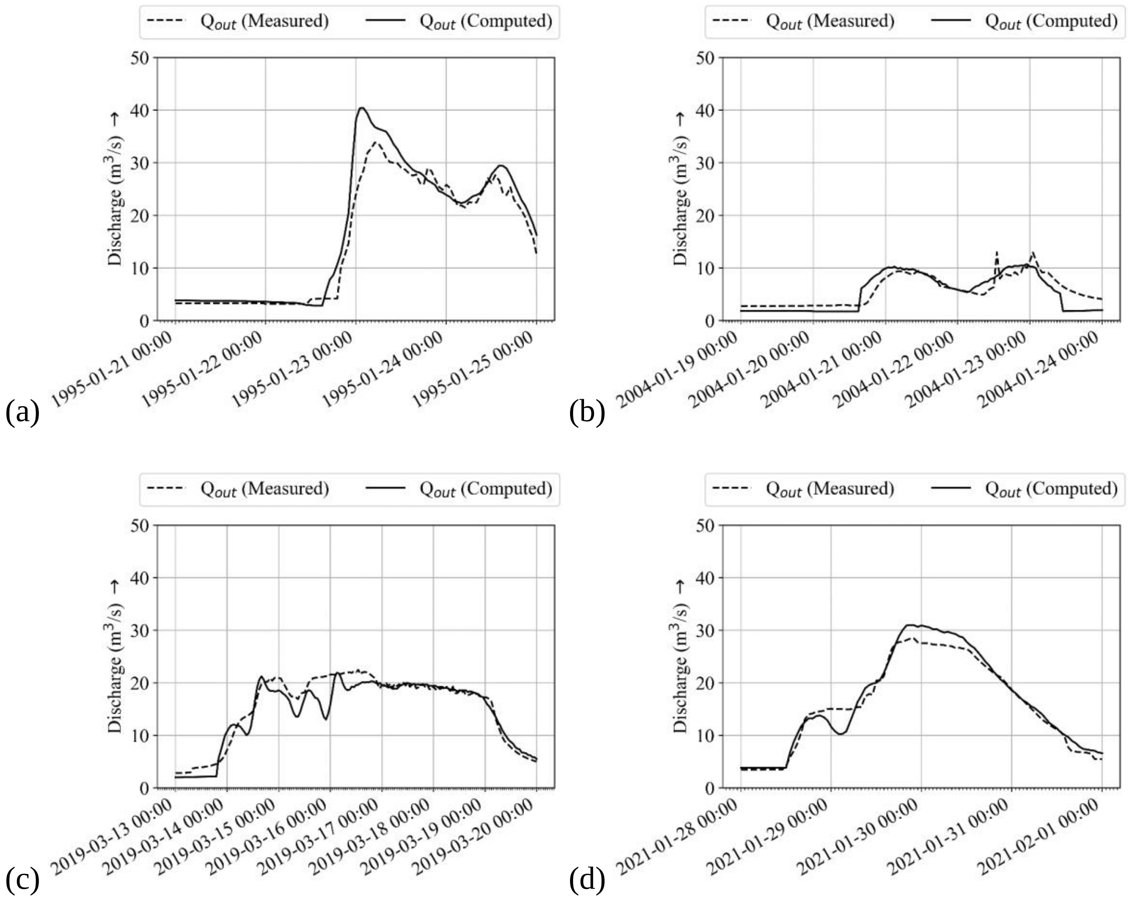

Figure 11: Outflow discharge ($Q_{out}$) v/s inflow discharge ($Q_{in}$) (peak values from each of the 18 events).

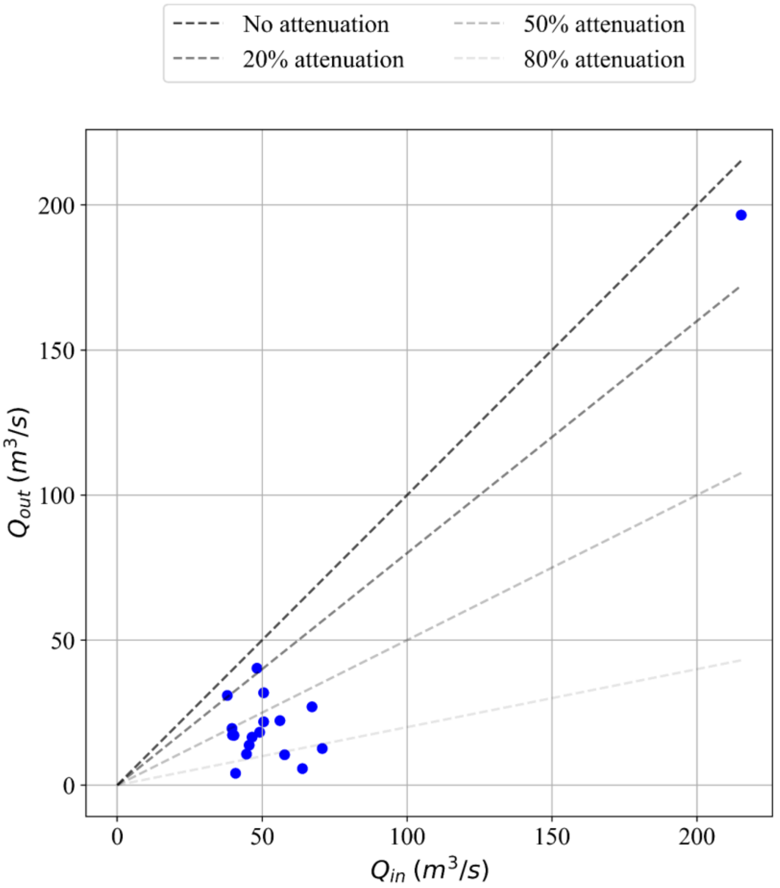


Figure 12: Plot of inflow and outflow hydrographs for all selected events over the days in a year.

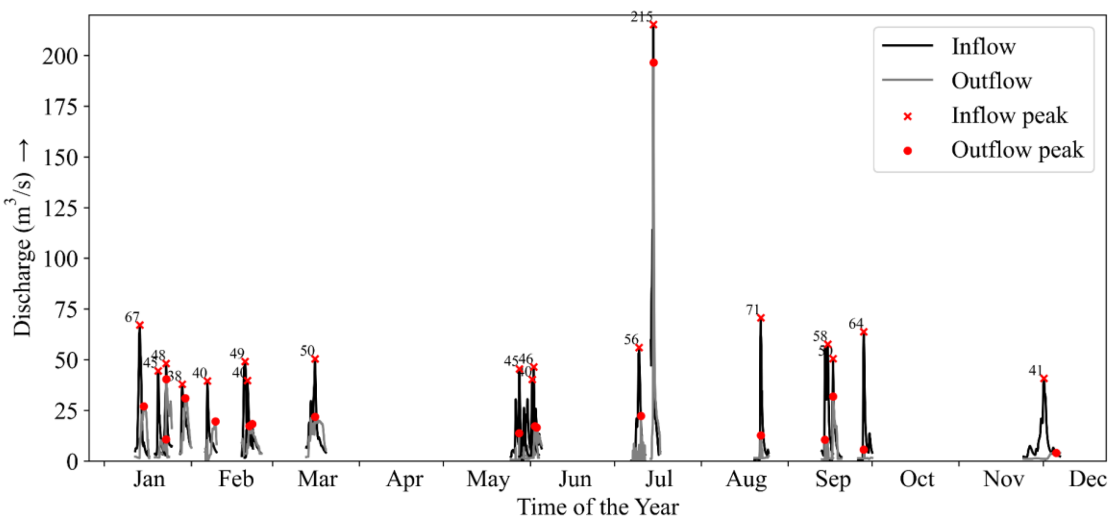

Figure 13: Comparison between inflow discharge ($Q_{in}$), outflow discharge ($Q_{out}$) and water level in the reservoir.

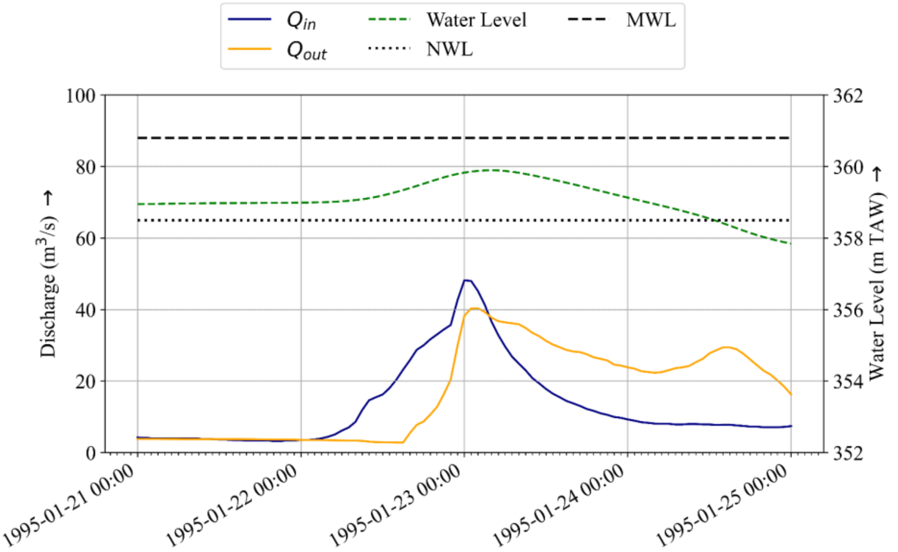


(a)

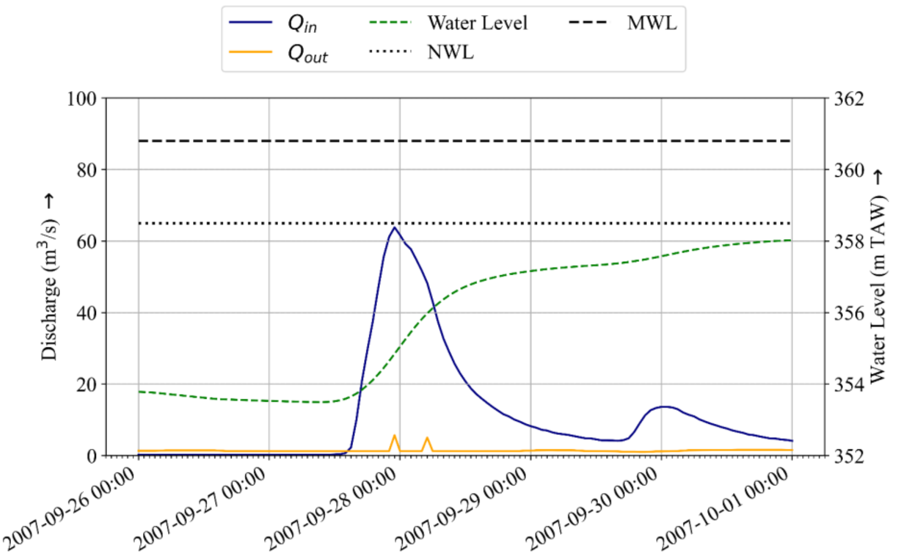


(b)

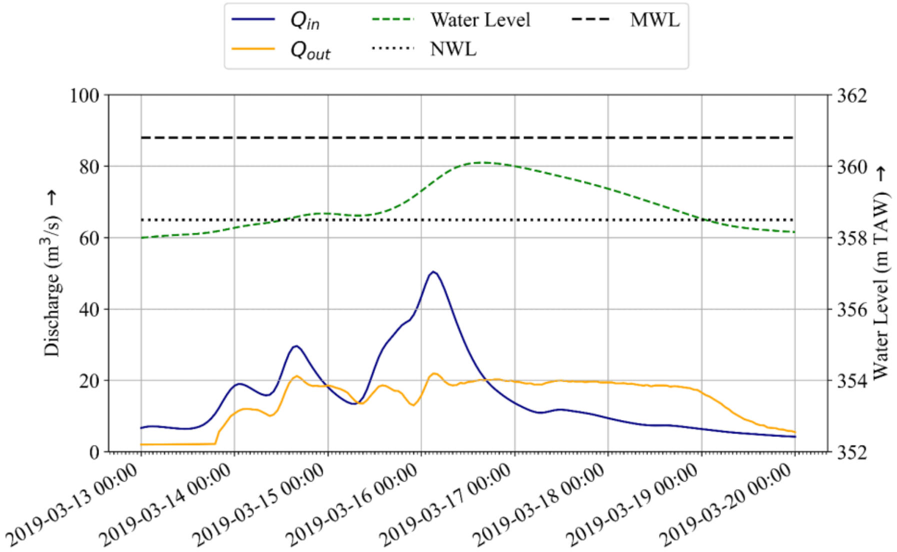

$Q_{in}$
$Q_{out}$
Water Level
NWL
MWL
Discharge (m³/s) →
Water Level (m TAW) →
100
80
60
40
20
0
362
360
358
356
354
352
2019-03-13 00:00
2019-03-14 00:00
2019-03-15 00:00
2019-03-16 00:00
2019-03-17 00:00
2019-03-18 00:00
2019-03-19 00:00
2019-03-20 00:00


(c)

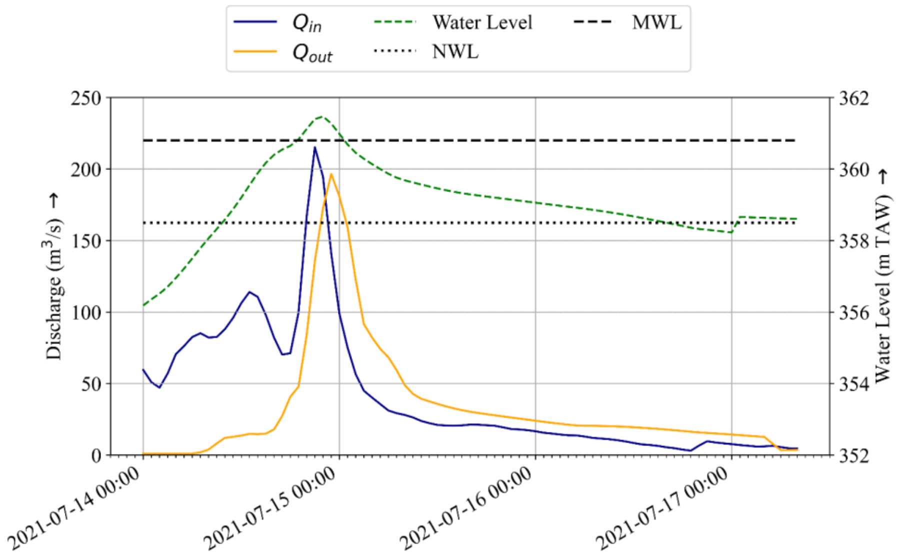

$Q_{in}$
$Q_{out}$
Water Level
NWL
MWL
Discharge (m³/s) →
Water Level (m TAW) →
250
200
150
100
50
0
362
360
358
356
354
352
2021-07-14 00:00
2021-07-15 00:00
2021-07-16 00:00
2021-07-17 00:00


(d)

Figure 14: Plot of peak attenuation ratio against the ratio of the cumulative incoming flood volume to the available volume in the reservoir. To avoid reducing the colour contrast between the other events' points, the range of the colour bar was not extended to the value of the peak inflow discharge of the 2021-07 event (about 215 $m^3/s$), which is represented in black.

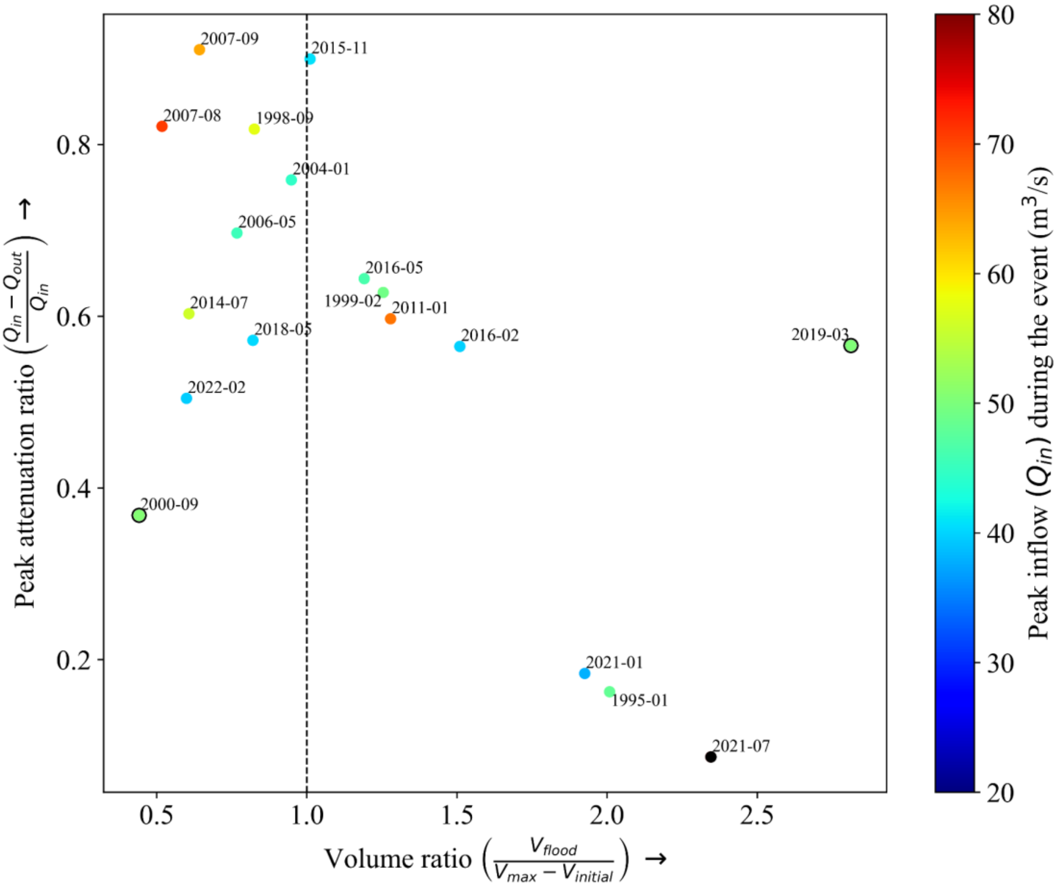

Figure 15: Comparison of time to peak for outflow and inflow discharge.

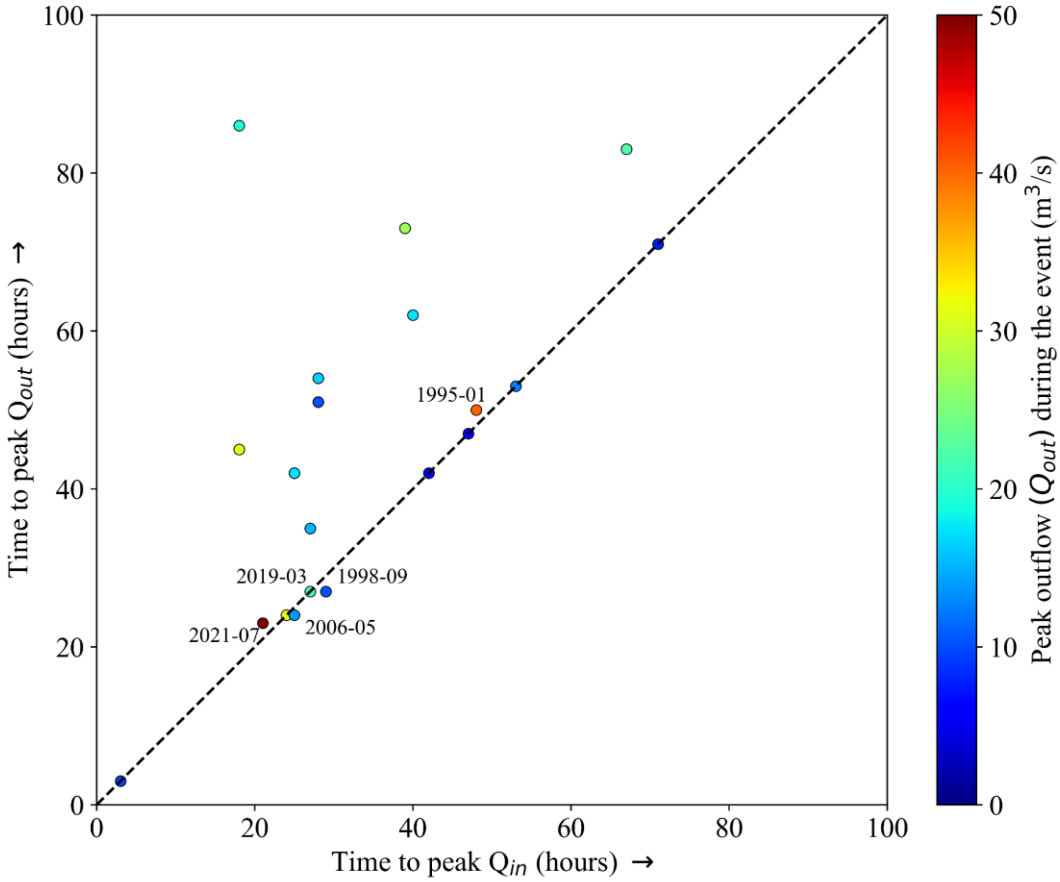

Figure 16: Plot of relative peak delay against the volume ratio of the event. The regression line is plotted not considering the three outliers.

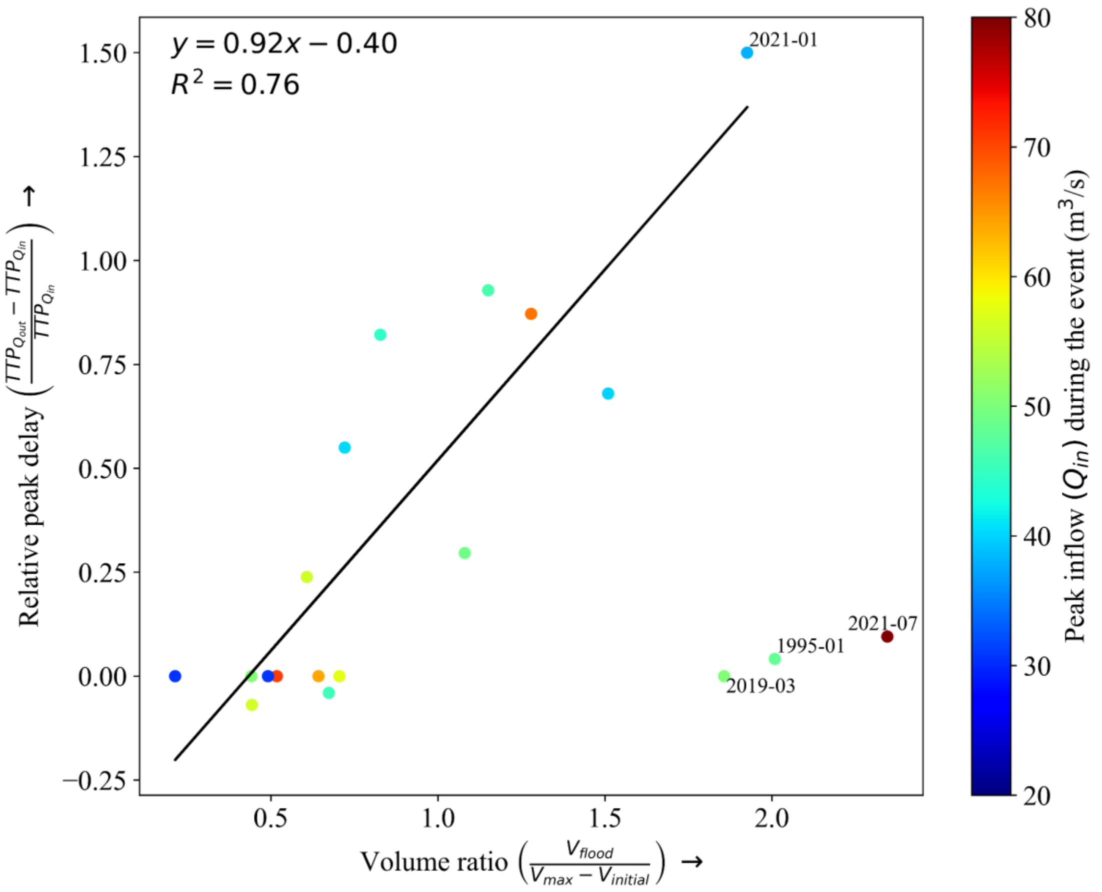

Figure 17: Comparison between maximum gradient for outflow and inflow discharge.

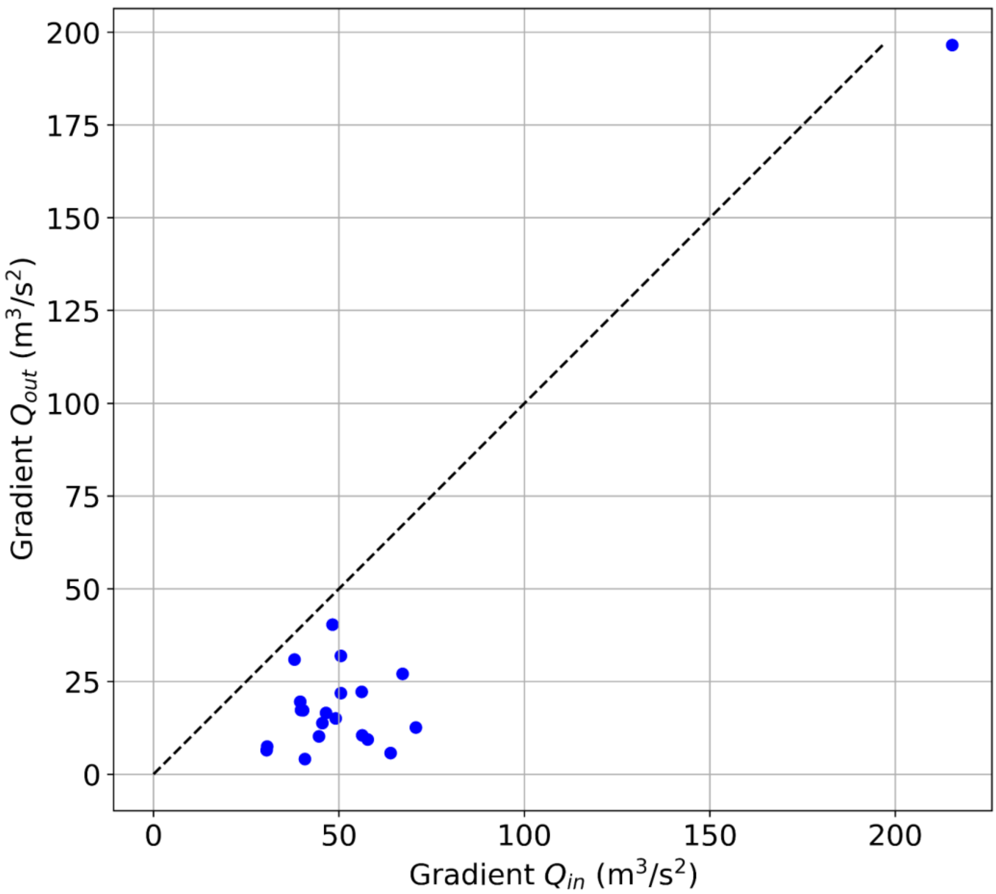

Figure 18: Cumulative inflow volume ($V_{in}$) vs cumulative outflow volume ($V_{out}$) for each major event.

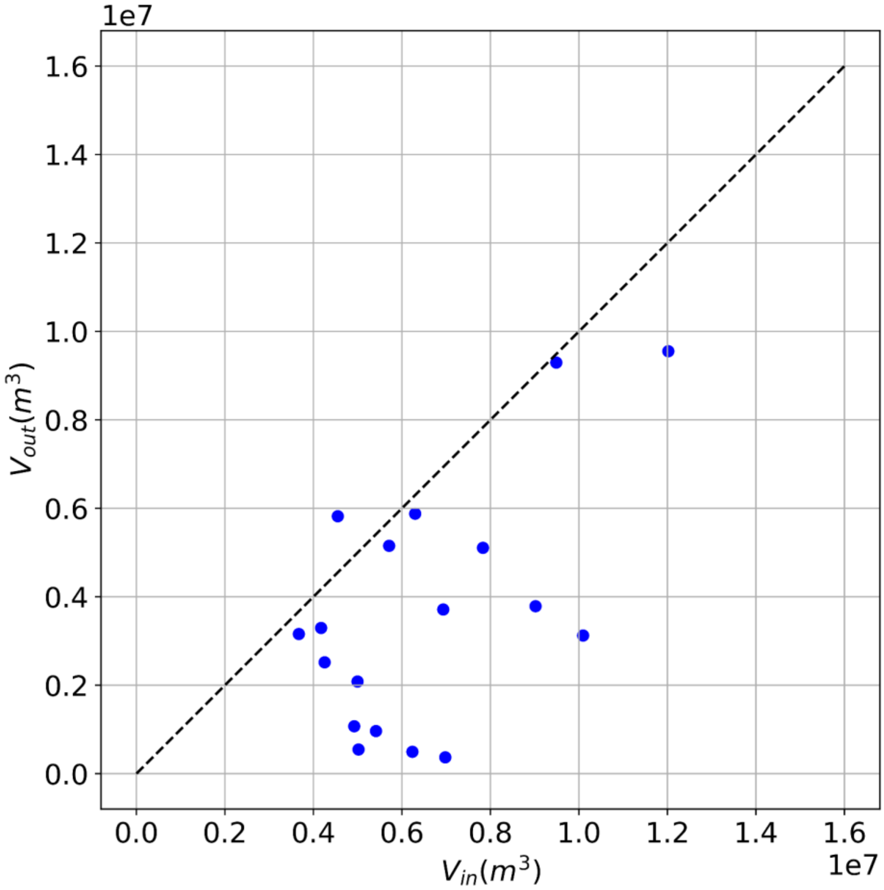

Figure 19: Plot of cumulative volume flowing in and out of the reservoir and the volume stored per event.

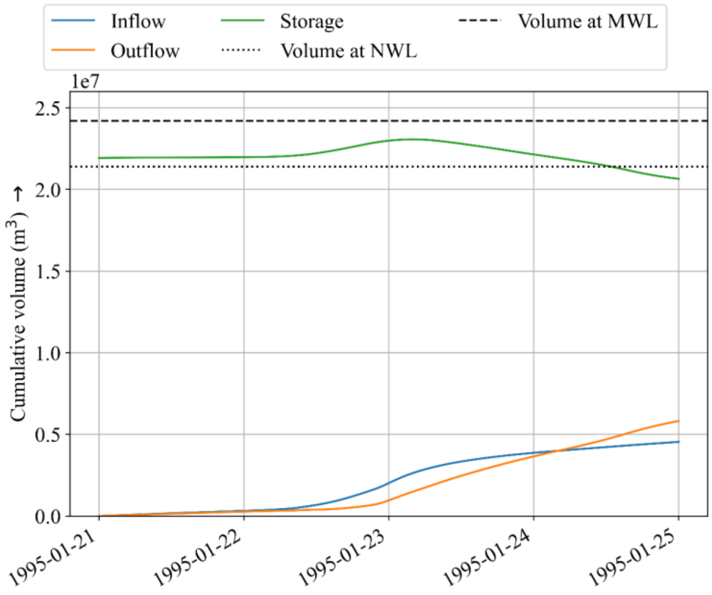


(a)

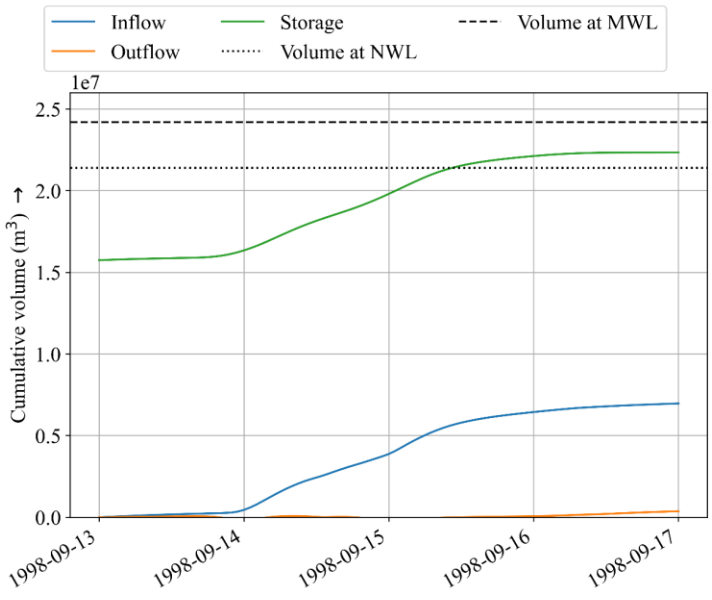


(b)

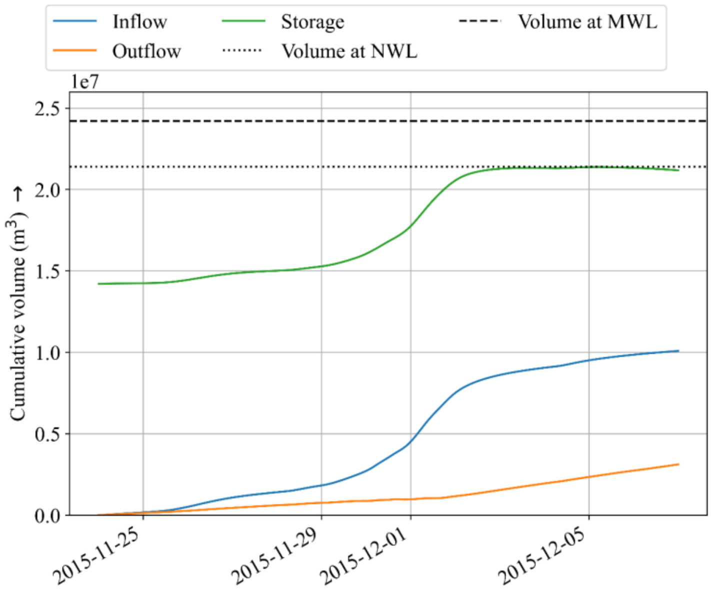
Inflow
Outflow
Storage
Volume at NWL
Volume at MWL
1e7
Cumulative volume (m3) →
2015-11-25
2015-11-29
2015-12-01
2015-12-05
(c)

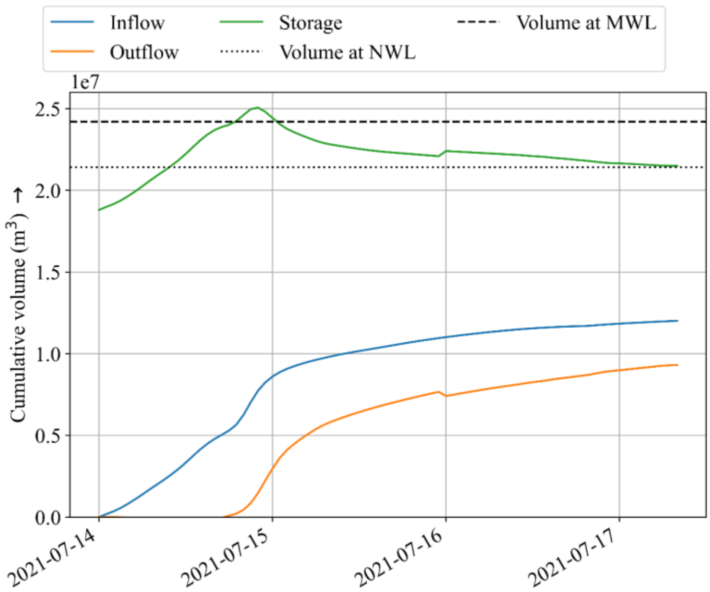
Inflow
Outflow
Storage
Volume at NWL
Volume at MWL
1e7
Cumulative volume (m3) →
2021-07-14
2021-07-15
2021-07-16
2021-07-17
(d)

Figure 20: Plot of the General Extreme Value (GEV) distribution fit (for inflow and outflow series)

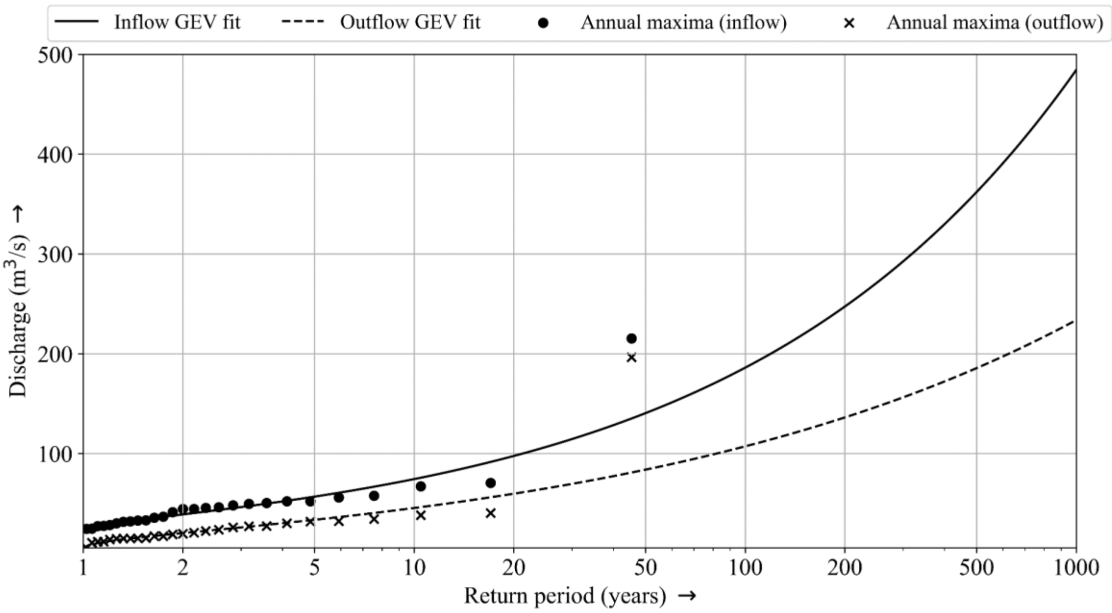


Figure 21: Relative reduction of discharges associated with floods of different return periods.

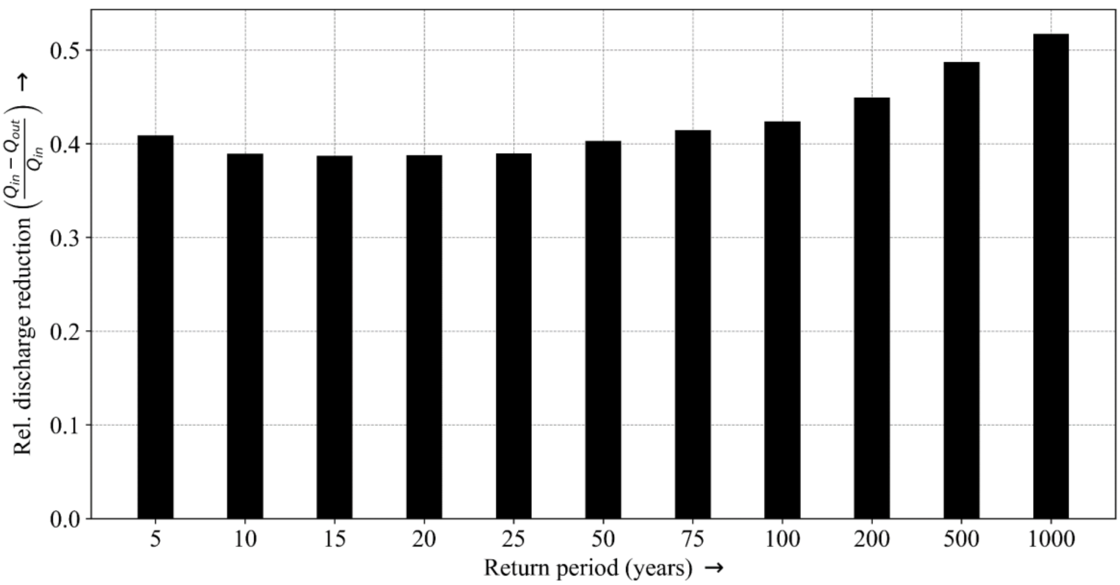

# A. Appendix

## *A.1. Reservoir water level during each hydrological year (1st October to 30th September) from 1995 to 2021, plotted over the days of a hydrological year.*

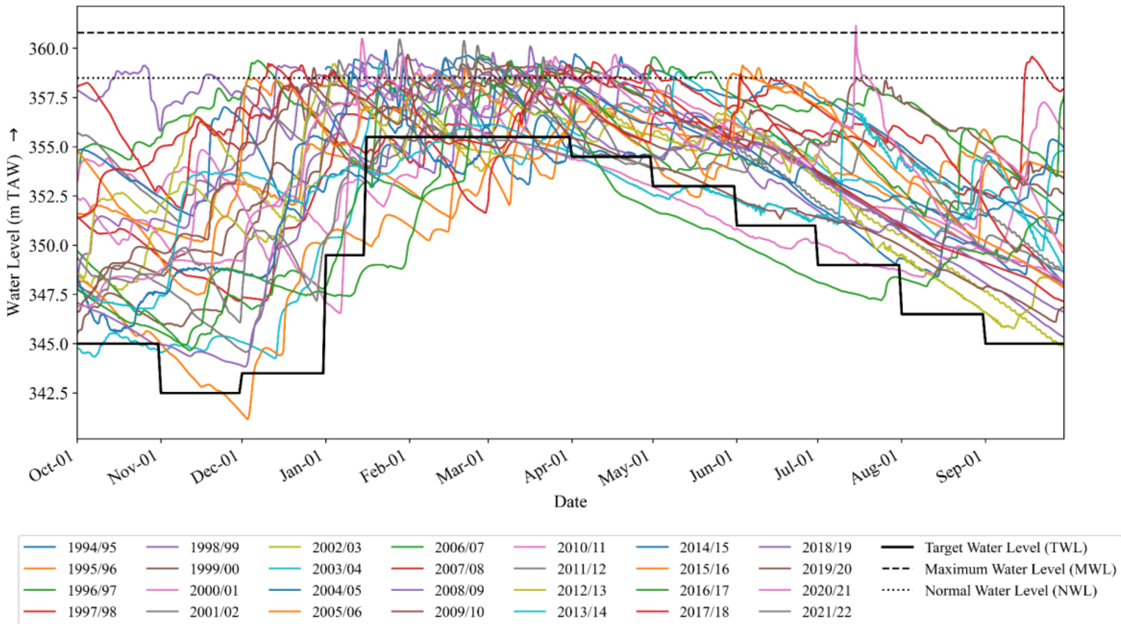


## *A.2. Effect of the Savitzky-Golay filter on inflow discharge data*

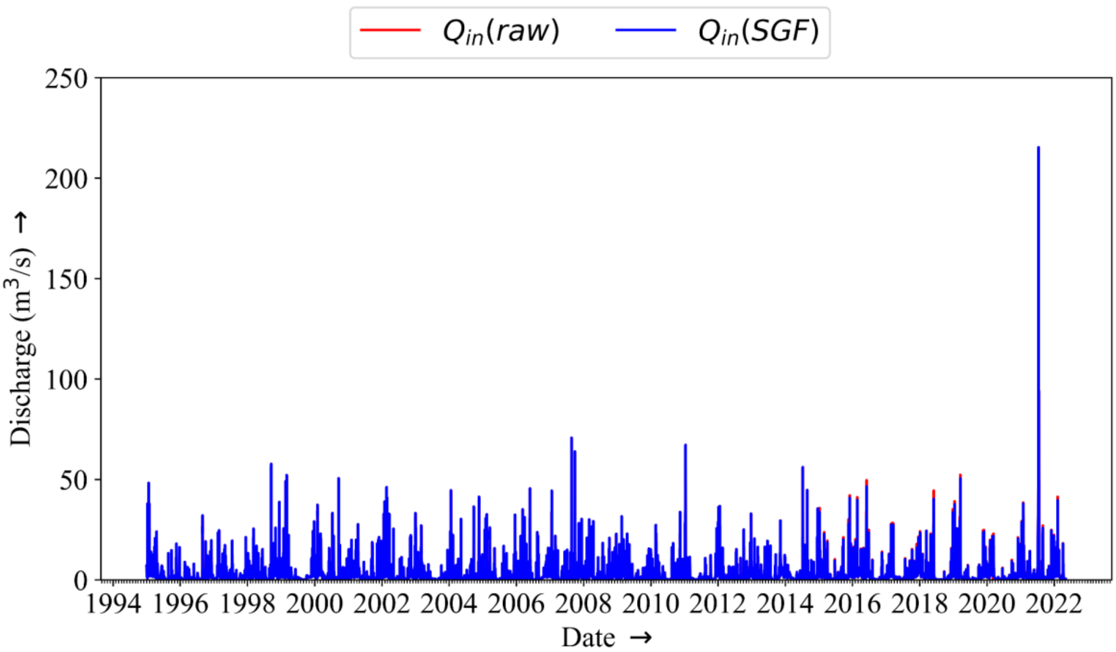

### *A.3. Stage-Volume curve for the Eupen reservoir*

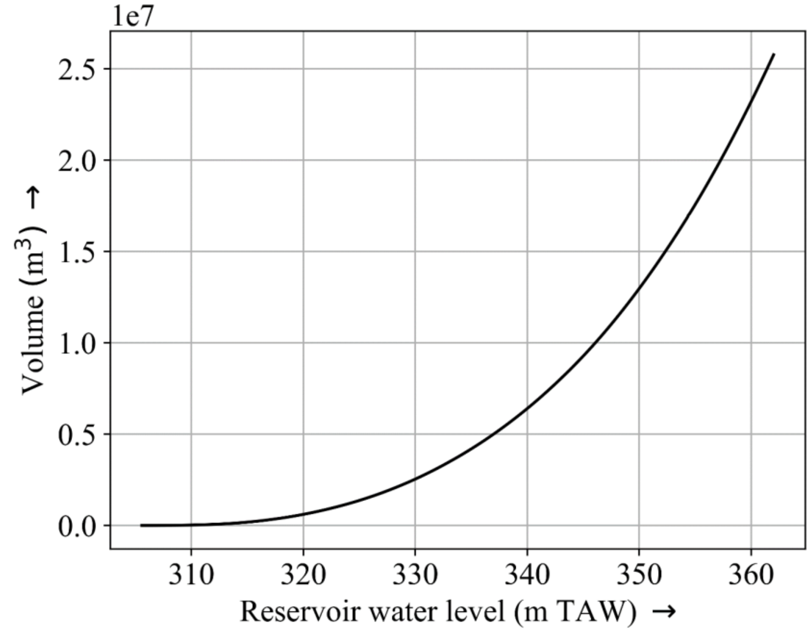


### *A.4. Comparison between measured and computed outflow discharge*

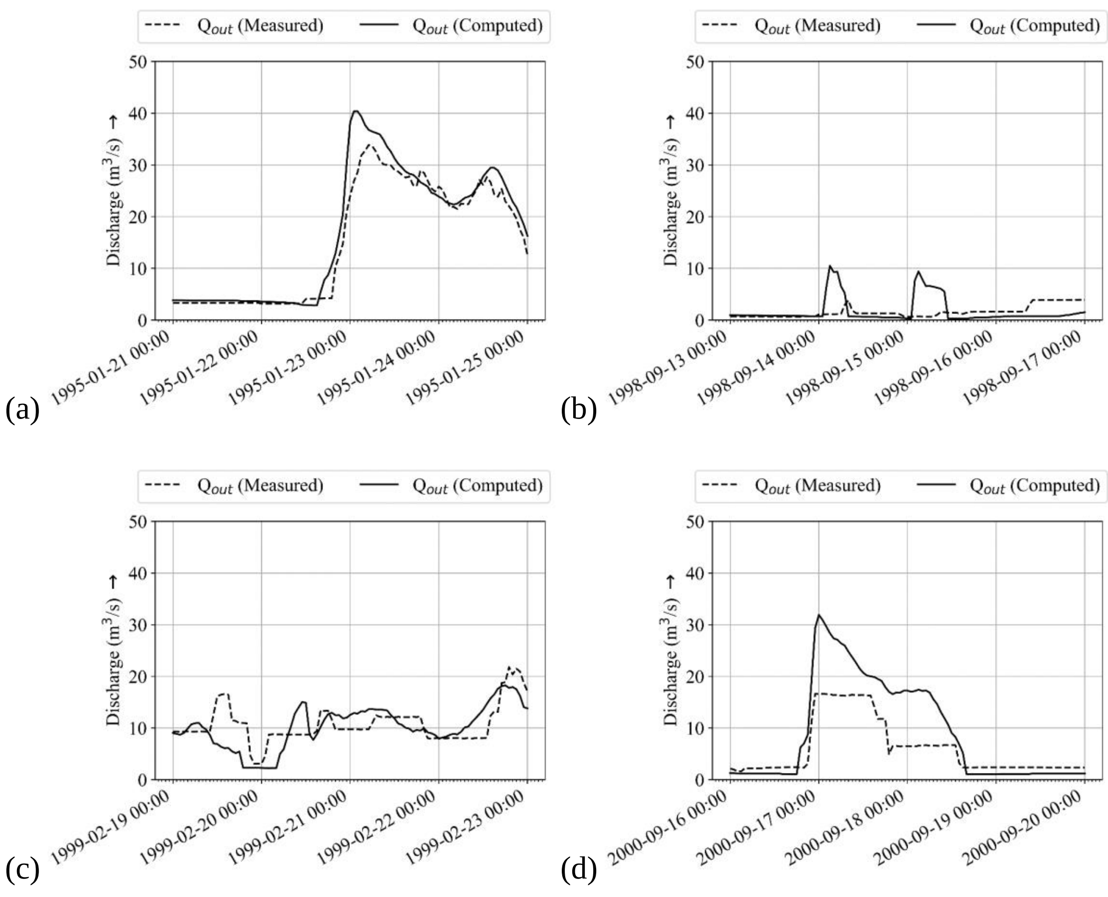

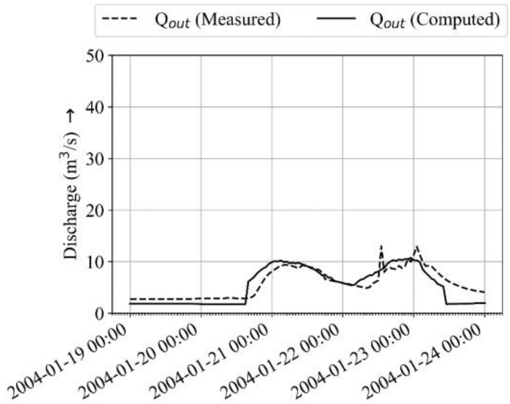
Q$_{out}$ (Measured)
Q$_{out}$ (Computed)
Discharge (m$^3$/s) →
2004-01-19 00:00
2004-01-20 00:00
2004-01-21 00:00
2004-01-22 00:00
2004-01-23 00:00
2004-01-24 00:00

(e)

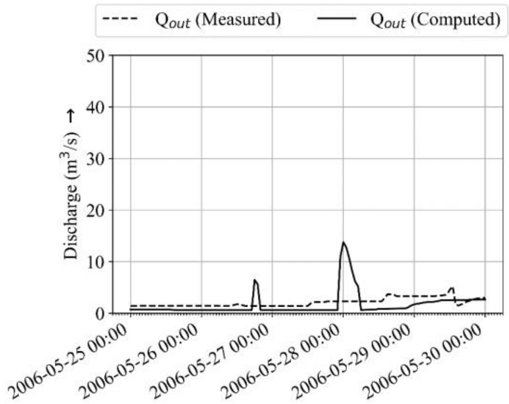
Q$_{out}$ (Measured)
Q$_{out}$ (Computed)
Discharge (m$^3$/s) →
2006-05-25 00:00
2006-05-26 00:00
2006-05-27 00:00
2006-05-28 00:00
2006-05-29 00:00
2006-05-30 00:00

(f)

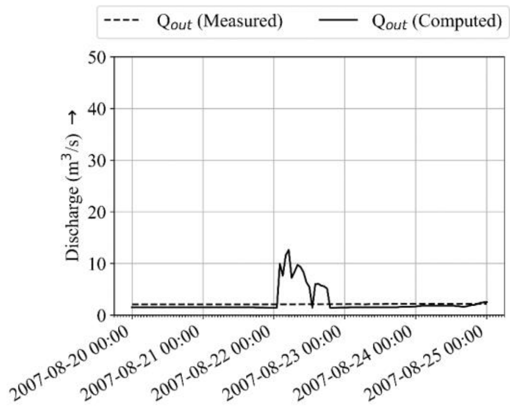
Q$_{out}$ (Measured)
Q$_{out}$ (Computed)
Discharge (m$^3$/s) →
2007-08-20 00:00
2007-08-21 00:00
2007-08-22 00:00
2007-08-23 00:00
2007-08-24 00:00
2007-08-25 00:00

(g)

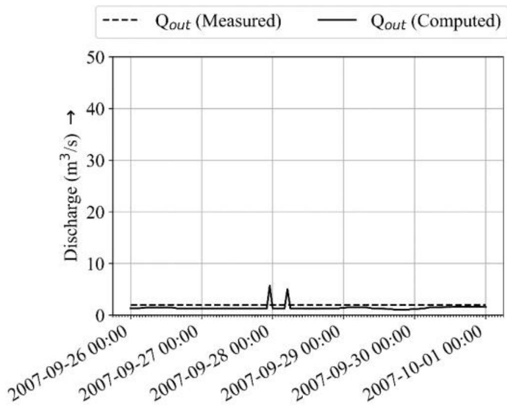
Q$_{out}$ (Measured)
Q$_{out}$ (Computed)
Discharge (m$^3$/s) →
2007-09-26 00:00
2007-09-27 00:00
2007-09-28 00:00
2007-09-29 00:00
2007-09-30 00:00
2007-10-01 00:00

(h)

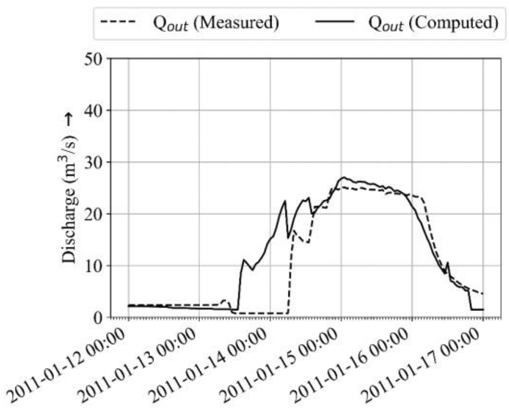
Q$_{out}$ (Measured)
Q$_{out}$ (Computed)
Discharge (m$^3$/s) →
2011-01-12 00:00
2011-01-13 00:00
2011-01-14 00:00
2011-01-15 00:00
2011-01-16 00:00
2011-01-17 00:00

(i)

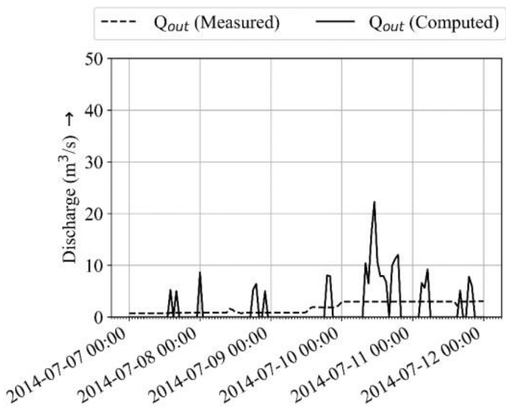
Q$_{out}$ (Measured)
Q$_{out}$ (Computed)
Discharge (m$^3$/s) →
2014-07-07 00:00
2014-07-08 00:00
2014-07-09 00:00
2014-07-10 00:00
2014-07-11 00:00
2014-07-12 00:00

(j)

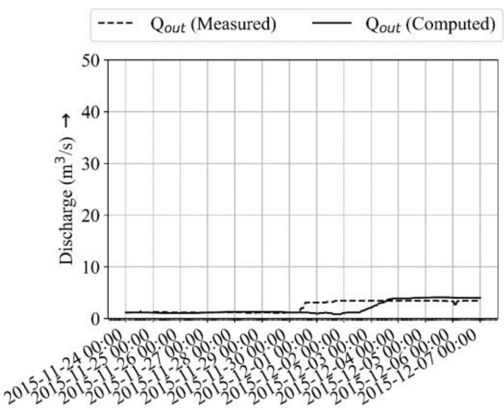
Q$_{out}$ (Measured)
Q$_{out}$ (Computed)
Discharge (m$^3$/s) →
2015-11-24 00:00
2015-12-07 00:00

(k)

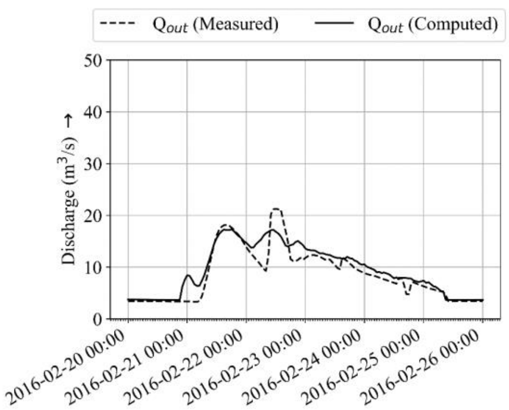
Q$_{out}$ (Measured)
Q$_{out}$ (Computed)
Discharge (m$^3$/s) →
2016-02-20 00:00
2016-02-21 00:00
2016-02-22 00:00
2016-02-23 00:00
2016-02-24 00:00
2016-02-25 00:00
2016-02-26 00:00

(l)

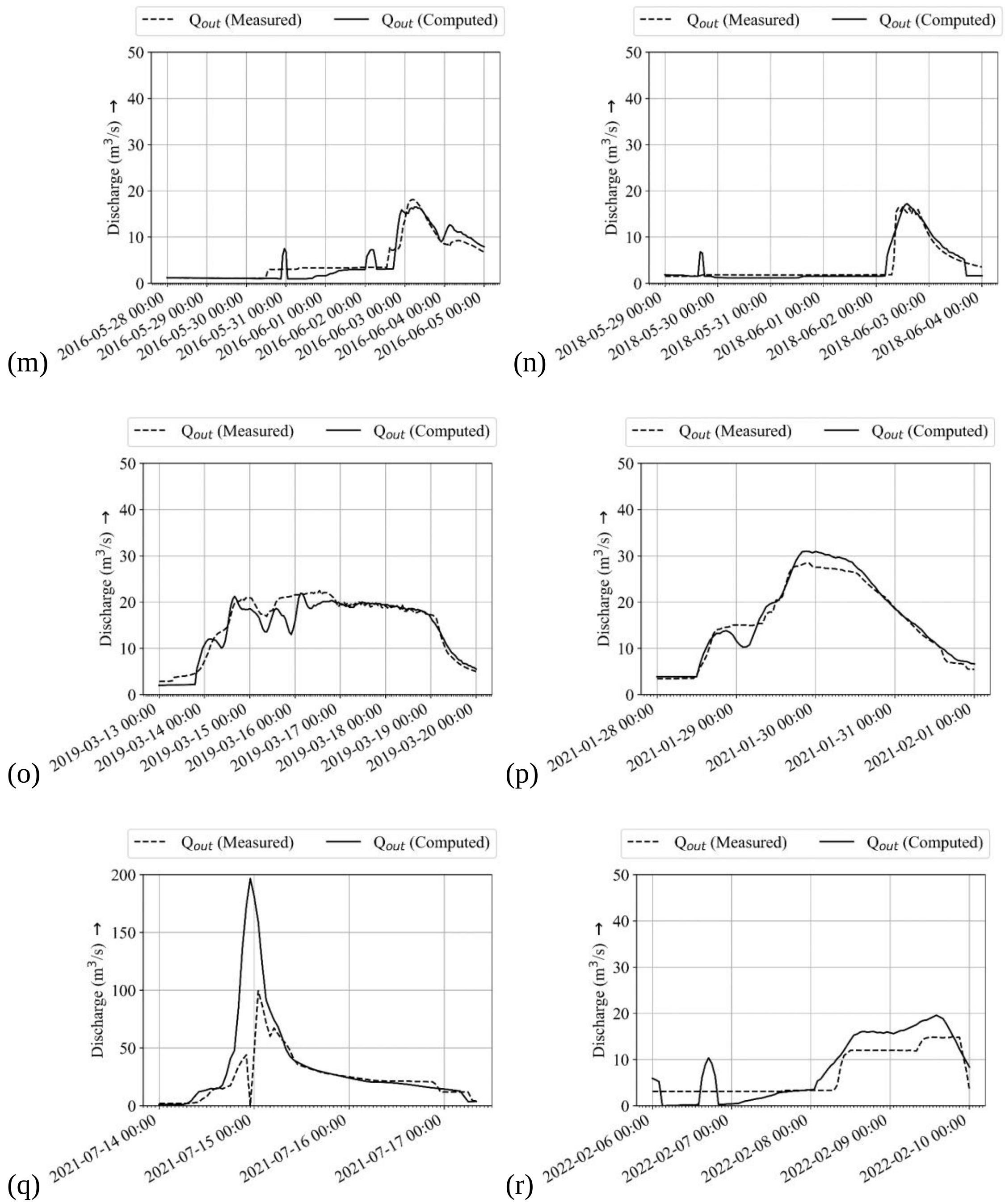
Q$_{out}$ (Measured)
Q$_{out}$ (Computed)
Discharge (m$^3$/s) →
(m)
2016-05-28 00:00
2016-05-29 00:00
2016-05-30 00:00
2016-05-31 00:00
2016-06-01 00:00
2016-06-02 00:00
2016-06-03 00:00
2016-06-04 00:00
2016-06-05 00:00
(n)
2018-05-29 00:00
2018-05-30 00:00
2018-05-31 00:00
2018-06-01 00:00
2018-06-02 00:00
2018-06-03 00:00
2018-06-04 00:00
(o)
2019-03-13 00:00
2019-03-14 00:00
2019-03-15 00:00
2019-03-16 00:00
2019-03-17 00:00
2019-03-18 00:00
2019-03-19 00:00
2019-03-20 00:00
(p)
2021-01-28 00:00
2021-01-29 00:00
2021-01-30 00:00
2021-01-31 00:00
2021-02-01 00:00
(q)
2021-07-14 00:00
2021-07-15 00:00
2021-07-16 00:00
2021-07-17 00:00
(r)
2022-02-06 00:00
2022-02-07 00:00
2022-02-08 00:00
2022-02-09 00:00
2022-02-10 00:00

## *A.5. Inflow vs outflow hydrographs for all considered flood events*

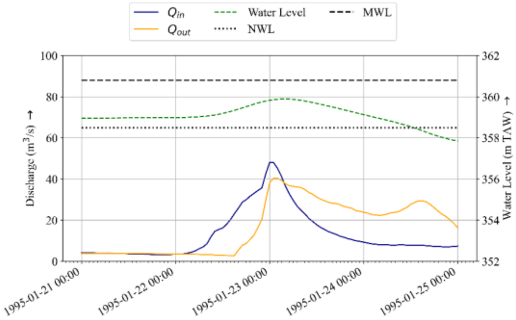


(a)

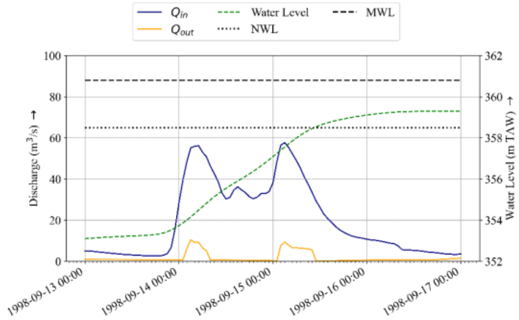


(b)

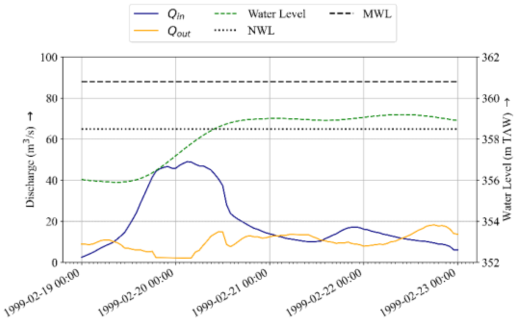


(c)

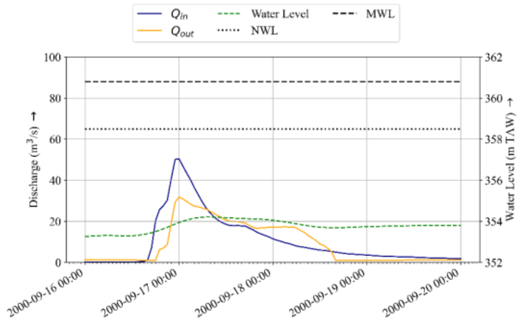


(d)

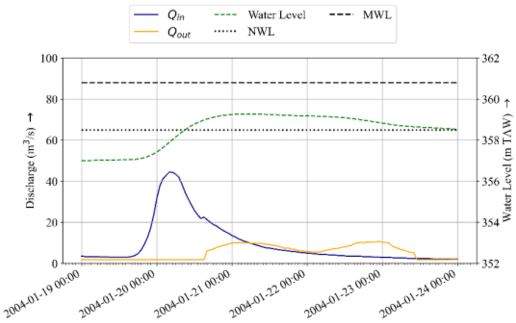


(e)

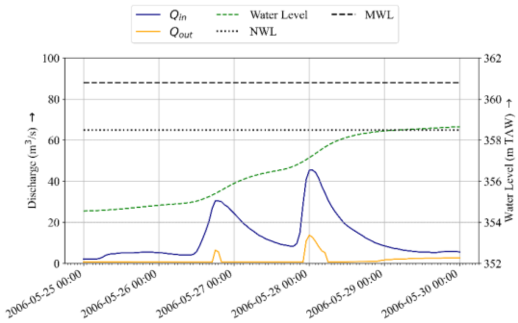


(f)

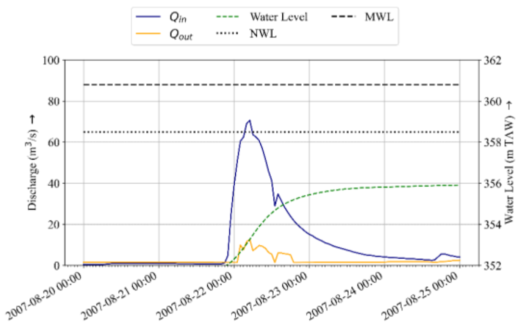


(g)

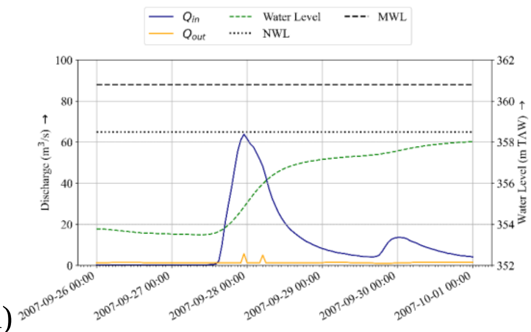


(h)

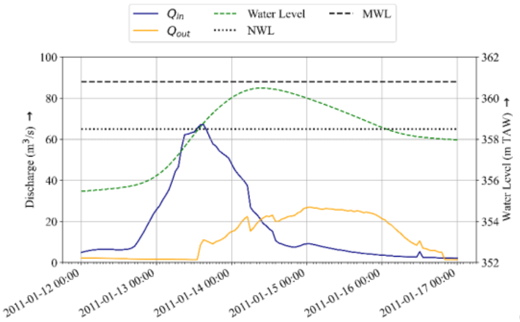
$Q_{in}$
$Q_{out}$
Water Level
NWL
MWL
Discharge (m³/s)
Water Level (m TAW)

(i)

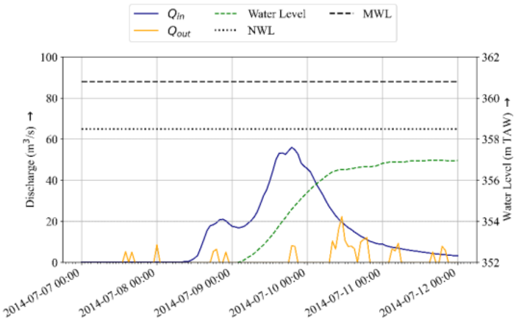
$Q_{in}$
$Q_{out}$
Water Level
NWL
MWL
Discharge (m³/s)
Water Level (m TAW)

(j)

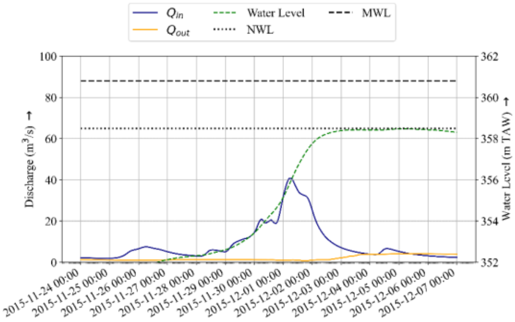
$Q_{in}$
$Q_{out}$
Water Level
NWL
MWL
Discharge (m³/s)
Water Level (m TAW)

(k)

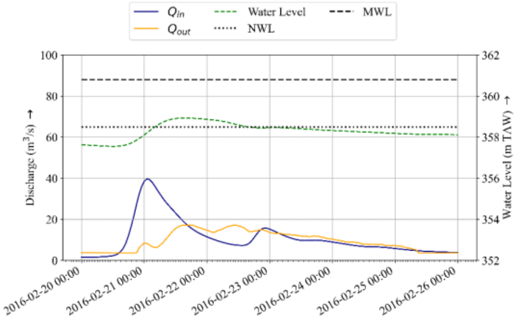
$Q_{in}$
$Q_{out}$
Water Level
NWL
MWL
Discharge (m³/s)
Water Level (m TAW)

(l)

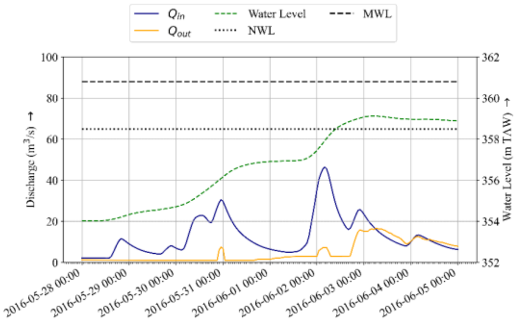
$Q_{in}$
$Q_{out}$
Water Level
NWL
MWL
Discharge (m³/s)
Water Level (m TAW)

(m)

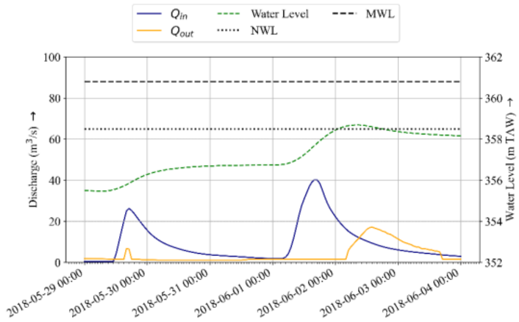
$Q_{in}$
$Q_{out}$
Water Level
NWL
MWL
Discharge (m³/s)
Water Level (m TAW)

(n)

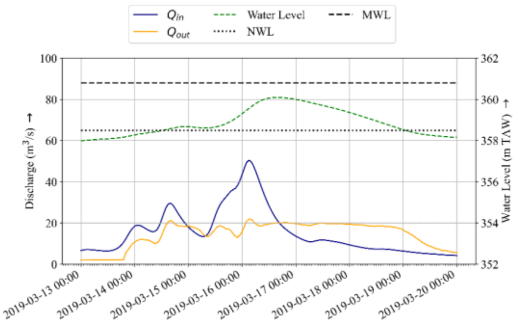
$Q_{in}$
$Q_{out}$
Water Level
NWL
MWL
Discharge (m³/s)
Water Level (m TAW)

(o)

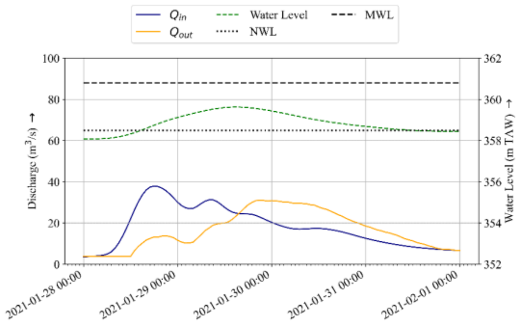
$Q_{in}$
$Q_{out}$
Water Level
NWL
MWL
Discharge (m³/s)
Water Level (m TAW)

(p)

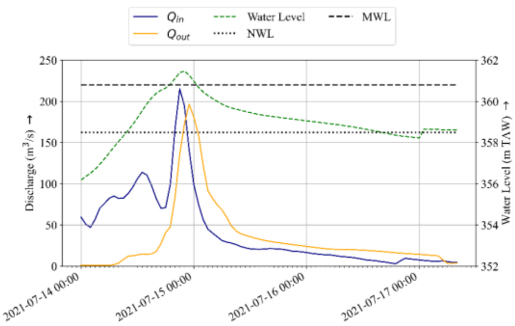
$Q_{in}$
$Q_{out}$
Water Level
NWL
MWL
Discharge (m³/s)
Water Level (m TAW)

(q)

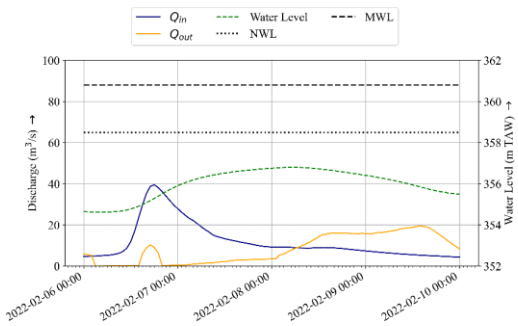
$Q_{in}$
$Q_{out}$
Water Level
NWL
MWL
Discharge (m³/s)
Water Level (m TAW)

(r)

### *A.6. Extended inflow, outflow, and water-level variation plot for the 1995-01 event*

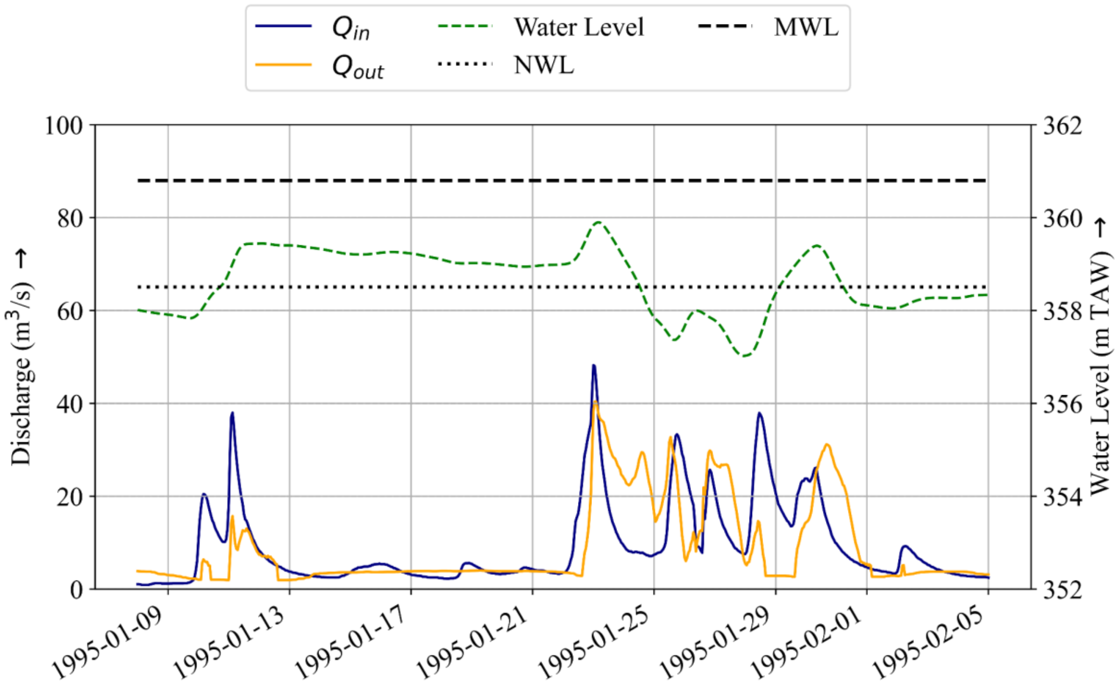

### A.7. *Peak inflow, peak outflow, total volume of flood and available reservoir volume corresponding to each event*

| Date | $Q_{in(\text{peak})}$ ($m^3/s$) | $Q_{out(\text{peak})}$ ($m^3/s$) | $V_{available}$ ($Mm^3$) | $V_{flood}$ ($Mm^3$) |
|---|---|---|---|---|
| 01-1995 | 48.21 | 40.37 | 2.27 | 4.5 |
| 09-1998 | 57.69 | 10.50 | 8.45 | 7.0 |
| 02-1999 | 49.10 | 18.28 | 5.53 | 6.9 |
| 09-2000 | 50.50 | 31.90 | 8.30 | 3.6 |
| 01-2004 | 44.55 | 10.74 | 4.49 | 4.2 |
| 05-2006 | 45.48 | 13.78 | 7.05 | 5.4 |
| 08-2007 | 70.70 | 12.64 | 9.51 | 4.9 |
| 09-2007 | 63.86 | 5.72 | 7.81 | 5.0 |
| 01-2011 | 67.14 | 27.05 | 6.12 | 7.8 |
| 07-2014 | 56.08 | 22.26 | 10.27 | 6.2 |
| 11-2015 | 40.80 | 4.09 | 9.99 | 10.0 |
| 02-2016 | 39.73 | 17.29 | 3.79 | 5.7 |
| 05-2016 | 46.45 | 16.55 | 7.57 | 9.0 |
| 05-2018 | 40.26 | 17.23 | 6.09 | 5.0 |
| 03-2019 | 50.46 | 21.91 | 3.38 | 9.5 |
| 01-2021 | 37.96 | 30.97 | 3.27 | 6.3 |
| 07-2021 | 215.27 | 196.60 | 5.57 | 12.0 |
| 02-2022 | 39.54 | 19.60 | 6.96 | 4.1 |

Notations are as follows: $Q_{in(\text{peak})}$ is the peak of the inflow discharge, $Q_{out(\text{peak})}$ the peak of the outflow discharge, $V_{available}$ is the available storage capacity in the reservoir at the start of the event, and $V_{flood}$ the volume of the flood wave.

## *A.8. Plot of the General Extreme Value (GEV) distribution fit (for inflow and outflow series) with different Confidence Interval(s) (C.I.).*